Λ single particle energies

Q. N. Usmani
Department of Physics, Faculty of Science and Environmental Studies, Universiti Putra Malaysia, 43400 UPM Serdang, Selangor, Malaysia

A. R. Bodmer
Physics Division, Argonne National Laboratory, Argonne, Illinois 60439-4843
and Department of Physics, University of Illinois at Chicago, Chicago, Illinois 60680

(Received 25 September 1998; published 22 October 1999)

The Λ single-particle energies B_Λ of hypernuclei (HN) are calculated microscopically using the Fermi hypernetted chain method to obtain for our ΛN and ΛNN potentials the Λ binding $D(\rho)$ to nuclear matter, and the effective mass $m^*_\Lambda(\rho)$ at densities $\rho \leqslant \rho_0$ (ρ_0 is normal nuclear density), and also the corresponding effective ΛN and ΛNN potentials. The Λ core-nucleus potential $U_\Lambda(r)$ is obtained by suitably folding these into the core density. The Schrödinger equation for U_Λ and m^*_Λ is solved for B_Λ. The fringing field (FF) due to the finite range of the effective potentials is theoretically required. We use a dispersive ΛNN potential but also include a phenomenological ρ dependence allowing for less repulsion for $\rho < \rho_0$, i.e., in the surface. The best fits to the data with a FF give a large ρ dependence, equivalent to an A dependent strength consistent with variational calculations of ${}^{5}_{\Lambda}$He, indicating an effective ΛNN dispersive potential increasingly repulsive with A whose likely interpretation is in terms of dispersive plus two-pion-exchange ΛNN potentials. The well depth is 29 ± 1 MeV. The ΛN space-exchange fraction corresponds to $m^*_\Lambda(\rho) \approx 0.75-0.80$ and a ratio of p- to s-state potentials of $\approx 0.5 \pm 0.1$. Charge symmetry breaking (CSB) is significant for heavy HN with a large neutron excess; with a FF the strength agrees with that obtained from the $A=4$ HN. The fits without FF are excellent but inconsistent with the requirement for a FF, with ${}^{5}_{\Lambda}$He, and also with the CSB sign for $A=4$.
[S0556-2813(99)04811-6]

PACS number(s): 21.80.+a, 21.10.Pc, 13.75.Ev, 11.30.Er

I. INTRODUCTION

In this paper we analyze the Λ single-particle (SP) separation energies B_Λ of Λ hypernuclei (HN) with a microscopic approach. The experimental SP energies have been obtained for a wide range of HN with (total) baryon number $A \leqslant 208$ and for orbital angular momenta up to $l_\Lambda = 3$ for large A [1,2]; in particular the recent data for La and Pb are very important for our results.

The Λ-nucleus potential roughly follows the density distribution $\rho(r)$ of the core nucleus and has an approximately constant value D_Λ in the interior of heavy HN. D_Λ is identified with the Λ binding in nuclear matter at normal nuclear density $\rho_0 = 0.165\,\mathrm{fm}^{-3}$. Then $B_\Lambda \approx D_\Lambda - T_\Lambda$ where the Λ kinetic energy $T_\Lambda \sim A^{-2/3}$. Table I shows the experimental B_Λ and Fig. 1 shows B_Λ vs $A^{-2/3}$. Extrapolation to $A \to \infty$, i.e., $A^{-2/3} \to 0$, in particular for the s_Λ states gives $D_\Lambda \approx 30$ MeV.

Microscopic calculations using variational Monte Carlo (VMC) techniques have been made for the $A \leqslant 5$ HN [3,4,5] and also for ${}^{17}_{\Lambda}$O [6], and D_Λ has been calculated with the Fermi hypernetted chain (FHNC) method [7,8] generalized to include ΛNN potentials [3]. However, for HN with $A > 5$ adequate variational techniques are in general not yet feasible and also not suitable for a more global approach.

We have therefore used an approach which depends centrally on variational FHNC calculations of the binding energy $D(\rho, k_\Lambda)$ of a Λ (momentum k_Λ) to nuclear matter (nm) of density ρ (for all $\rho \leqslant \rho_0$), and of the associated ΛN and ΛNN effective potentials $\tilde{V}_{\Lambda N}$ and $\tilde{V}_{\Lambda NN}$. The latter are then appropriately folded into the density $\rho(r)$ of the core nucleus to give a SP potential $U_\Lambda(r)$, while the k_Λ dependence of D gives the effective mass $m^*_\Lambda(r)$. These are then used in a Schrödinger equation to obtain the B_Λ. Core distortion is quite small for the relevant A [9].

Our approach thus has important elements of a local-density approximation but goes beyond this. Our effective interactions are (slightly) ρ dependent since they involve ΛN and ΛNN correlations, which depend on ρ. In the leading order of the cluster expansion, our effective ΛN potential corresponds closely to a Brueckner-Hartree-Fock approach which uses the (ρ-dependent) G matrix in the leading order

TABLE I. Experimental B_Λ (MeV).

HN	$B_\Lambda(s)$	$B_\Lambda(p)$	$B_\Lambda(d)$	$B_\Lambda(f)$
${}^{11}_{\Lambda}$B	10.2±0.07			
${}^{12}_{\Lambda}$C	10.8±0.01	0.1±0.5		
${}^{13}_{\Lambda}$C	11.7±0.01	0.8±0.5		
${}^{16}_{\Lambda}$O	12.5±0.35	2.5±0.5		
${}^{28}_{\Lambda}$Si	16.0±0.3	7.0±1		
${}^{32}_{\Lambda}$S	17.5±0.5	8.1±0.6		
${}^{40}_{\Lambda}$Ca	18.7±1.1	11.0±0.6	1.0±0.5	
${}^{51}_{\Lambda}$V	19.9±1.0		4.0±0.5	
${}^{89}_{\Lambda}$Y	22.1±1.6	16.0±1	9.5±1	2.5±1
${}^{139}_{\Lambda}$La	23.8±1	20.1±0.4		
${}^{208}_{\Lambda}$Pb	26.5±0.5	21.3±0.7		

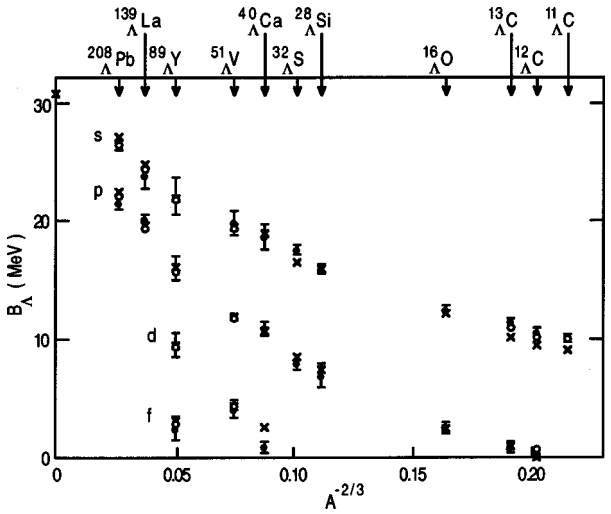

FIG. 1. B_Λ vs $A^{-2/3}$ for the designated l values. (1) The experimental B_Λ are shown as full circles with error bars. (2) The calculated B_Λ for $V_0=6.2$ MeV, $W=0.021$ MeV, $\beta=2$, $\epsilon=0.255$ are shown as crosses. (3) The calculated B_Λ for ${}^{51}_{\Lambda}$V,${}^{89}_{\Lambda}$Y,${}^{139}_{\Lambda}$La,${}^{208}_{\Lambda}$Pb for the same parameters as in (2) but including CSB ($V_0^{\rm CSB}=-0.05$ MeV) are shown as open circles. (4) The calculated B_Λ for ${}_{\Lambda}$C for the same parameters as in (2) except that $\beta=0.1$, are also shown as open circles.

of a reaction-matrix approach; but our approach goes beyond this since we make an ''exact'' FHNC calculation which treats exactly the clusters of all orders except for the elementary diagrams which are negligible for a dilute system such as normal nuclear matter. As demonstrated in Sec. III our effective $\tilde{V}_{\Lambda N}$ is quite close to that obtained in the leading order of the cluster expansion. For soft direct (no space exchange) potentials for which the ΛN correlations are weak, our approach is equivalent to the Hartree approximation, except for the neglect of core distortion. Similarly, for a dispersive type $V_{\Lambda NN}$ [Eq. (6)] the effective $\tilde{V}_{\Lambda NN}$ is well approximated by the leading order of the cluster expansion and is again exact in the limit of the Hartree approximation. Space-exchange potentials give some nonlocality (as in HF) and our principal approximation is the use of a local $m^*_\Lambda[\rho(r)]$; this should be a reasonable approximation but needs further investigation. Our procedure should then be a good approximation to an exact microscopic treatment and provides a theoretically well-founded phenomenology. Folding the effective potentials into the core density is an essential element and is necessary to obtain a realistic SP potential, with the associated fringing field (FF) due to the finite range of the ΛN and ΛNN potentials being a crucial component.

The smallness of the core polarization provides a great simplification since the core nucleus can be treated to a good approximation as undistorted. Elsewhere we have shown that even for quite moderate A, core polarization gives a very small increase $\Delta B_\Lambda \lesssim 0.2$ MeV [9]. For a very light HN such as ${}^{5}_{\Lambda}$He the correct treatment of core polarization involves a rearrangement energy which depends essentially on ΛN correlations but which is expected to be unimportant for larger A; even for ${}^{5}_{\Lambda}$He core polarization contributes $\lesssim 0.4$ MeV [10].

There are two further new features of our work.

(1) Our treatment of ΛNN forces is more phenomenological than in our earlier work [11] which included dispersive ($V^D_{\Lambda NN}$) and two-pion exchange ($V^{2\pi}_{\Lambda NN}$) ΛNN forces in the calculation of D. However, the FHNC calculation for $V^{2\pi}_{\Lambda NN}$ was not and still has not been adequately implemented since existing calculations cannot reproduce the feature of VMC calculations of light HN [3–6] for which ΛNN correlations give a much reduced repulsive or even an attractive contribution. For $V^D_{\Lambda NN}$ there is no such problem as the correlations are well under control, and a repulsive contribution is always obtained with both VMC and FHNC calculations. We therefore use only a dispersive type $V_{\Lambda NN}$ but allow for a possible A dependence of this due to $V^{2\pi}_{\Lambda NN}$ (as well as to a possible A-dependent $V^D_{\Lambda NN}$) through an additional phenomenological ρ dependence which makes $V_{\Lambda NN}$ less repulsive for $\rho<\rho_0$. Since lighter nuclei have relatively more surface, this translates (Sec. V) into an increasingly repulsive ΛNN contribution for larger A.

(2) We include a charge symmetry breaking (CSB) component in the ΛN potential. We consider CSB strengths comparable to that obtained from the $A=4$ HN [12]. For heavy HN with a substantial neutron excess the CSB contribution is moderate but significant (Sec. VI); in particular the recent data for La and Pb are essential for a significant determination of the CSB potential.

Previous calculations of the SP B_Λ have used various approaches. Ours is perhaps closest to that of Millener *et al.* [13] who in addition to an analysis based on a phenomenological $D(\rho)$ (also Ref. [14]) also considered a local density approximation based on phenomenological zero-range Skyrme forces. Many salient features were already demonstrated in this paper: in particular the ''saturation'' property of $D(\rho)$ resulting from the need for strongly repulsive ΛNN forces, as well as that for $m^*_\Lambda<m_\Lambda$. However, as also in our earlier work [11], finite range effects, i.e., the FF, were not adequately included. Relativistic mean-field calculations [15] give a surprisingly good fit with only a very few parameters, the FF being implicitly included (through the meson fields); however, RMFT is not a microscopic approach and cannot be directly related to the ΛN and ΛNN forces. Brueckner-Hartree-Fock type calculations [16,17] have been made with ρ-dependent G matrices calculated for various OBE potentials [18,19] which include $\Lambda N-\Sigma N$ coupling, the suppression of the latter in nuclear matter first shown by realistic G-matrix calculations in Ref. [20] being roughly equivalent to a dispersive $V_{\Lambda NN}$. Unfortunately, higher order contributions including the two-pion-exchange ΛNN contribution, have so far not been estimated.

A brief outline of the paper follows. Section II discusses our potentials, including CSB. Section III presents our theoretical procedure. Section IV discusses our fits to the data, including the dependence of χ^2 on our potential parameters which is systematically explored. Section V discusses the A and ρ dependence of the effective ΛNN potential. Section VI

discusses our fits with CSB. Section VII summarizes results, in particular our best fits.

II. Λ-NUCLEAR INTERACTIONS

A. ΛN potential

Charge symmetric potential. Since the Λ has isospin $I=0$ there is no (strong) $\Lambda\Lambda\pi$ vertex, and hence no OPE potential. However, isospin allows a $\Lambda\Sigma\pi$ vertex. The two-pion-exchange (TPE) potential is then a dominant part of the ΛN potential and is dominated by the strong tensor OPE component acting twice. There will also be K, K^* exchange potentials which will, in particular, contribute to the space-exchange and the ΛN tensor potentials. The latter are of quite short-range and furthermore are also quite weak because the K and K^* tensor contributions are of opposite signs [19,21]. Also there will be short-range contributions from ω, quark-gluon-exchange, etc., which we represent with a short-range Saxon-Wood repulsive potential which, somewhat arbitrarily, we take to be very nearly the same as for the NN potential [22].

We then use an Urbana-type central potential [3,22] with space exchange and consistent with Λp scattering. We need only the spin-average potential which is

$$V_{\Lambda N}(r)=V(r)+V^x_{\Lambda N}, \quad V^x_{\Lambda N}=\epsilon V(r)(1-P_x). \tag{1}$$

The direct potential is

$$V(r)=W_0[1+\exp\{(r-R)/a\}]^{-1}-V_{2\pi}, \quad V_{2\pi}=V_0T^2_\pi(r), \tag{2}$$

where $W_0=2137$ MeV, $R=0.5$ fm, $a=0.2$ fm, and r is in fm. $T_\pi(r)$ is the one-pion-exchange tensor potential shape modified with a cutoff

$$T_\pi(r)=(1+3/x+3/x^2)(e^{-x}/x)(1-e^{-cr^2})^2, \tag{3}$$

with $x=0.7r$ and $c=2.0\,\mathrm{fm}^{-2}$. The Λp scattering at low energies is then well fitted with $V_0=6.15\pm0.05$ MeV. $V^x_{\Lambda N}$ is the space-exchange potential and P_x is the ΛN space-exchange operator. The exchange fraction ϵ determines the strength of $V^x_{\Lambda N}$ relative to the direct potential; ϵ is quite poorly determined from the Λp forward-backward asymmetry to be $\epsilon\approx0.1-0.38$. ϵ determines the odd-state potential; thus the p-state potential is

$$V_p=(1-2\epsilon)V(r) \quad \text{or} \quad V_p/V_s=1-2\epsilon. \tag{4}$$

Charge symmetry breaking potential. This is expected on theoretical grounds and is also required by the data, in particular the ground and excited state energies of ${}^4_\Lambda$H and ${}^4_\Lambda$He. These were analyzed in Ref. [12] with a phenomenological spin-dependent CSB potential and using central NN forces. It was found to be effectively spin independent. (Any appreciable spin dependence would in any case give only a very small contribution for large A relative to the spin-independent term.) The CSB potential we use is then to be added to the attractive part $V_{2\pi}$ of Eq. (2); its spin-independent part is

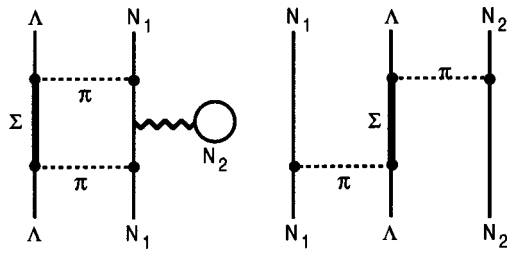

FIG. 2. Diagrams for dispersive and two-pion-exchange ANN potentials.

$$V^{\mathrm{CSB}}_{\Lambda N}=\tau_3V^{\mathrm{CSB}}_0T^2_\pi(r), \tag{5}$$

where analysis of the $A=4$ HN gives $V^{\mathrm{CSB}}_0\simeq-(0.05\pm0.005)$ MeV. The negative sign corresponds to a more attractive Λp than Λn potential. CSB makes a relatively small but significant contribution for the heaviest HN with an appreciable neutron excess.

B. ΛNN potentials

With only a ΛN potential fitted to Λp scattering the heavier HN are strongly overbound. Many-body effects for a central $V_{\Lambda N}$ can arise through changes in the ΛN correlation function $g_{\Lambda N}$ due to the presence of other nucleons. However, such effects are quite small as shown in Sec. III. Suppression of a ΛN tensor force by other nucleons is also expected to be quite small, both because of its short range and weakness [23]. However, the TPE ΛN potential $V_{2\pi}$ can be quite strongly suppressed because of modifications of the propagation of the intermediate Σ or N by other nucleons (Fig. 2). Coupled-channel reaction-matrix calculations can give a large repulsive contribution because of the large (mostly OPE tensor) couplings together with the small $\Sigma-\Lambda$ mass difference [20,24]. We represent such suppression effects by a phenomenological (repulsive) ''dispersive'' ΛNN potential of the form

$$V_{\Lambda NN}\equiv V^D_{\Lambda NN}=WT^2_\pi(r_{\Lambda1})T^2_\pi(r_{\Lambda2}), \tag{6}$$

where $r_{\Lambda i}$ are the Λ-nucleon separations. A strength $W\approx0.01-0.02$ MeV gives a repulsive contribution roughly consistent with the suppression obtained in coupled-channel reaction matrix calculations. Both VMC calculations of light HN and FHNC calculations of $D(\rho)$ always give repulsion (for $W>0$).

TPE ΛNN forces (Fig. 2) arise from a p-wave pion interaction of the Λ with each of two nucleons [25,26]. The corresponding potential $V^{2\pi}_{\Lambda NN}$ is noncentral with tensor components and is angle dependent (between $\vec{r}_{1\Lambda}$ and $\vec{r}_{2\Lambda}$). It has been used together with $V^D_{\Lambda NN}$ in VMC calculations for $A\leqslant5$, in particular of ${}^5_\Lambda$He [3–5] and of ${}^{17}_\Lambda$O [6]. With appropriate ΛNN correlations (including tensor and angle-dependent ΛNN correlations) the contribution of $V^{2\pi}_{\Lambda NN}$ can then be quite strongly attractive. This was already shown in earlier calculations with central NN forces [3]. Calculations with more realistic NN forces [27], in which case the tensor components of $V^{2\pi}_{\Lambda NN}$ also contribute, give an even more at-

tractive contribution. Thus the net contribution of $V^D_{\Lambda NN} + V^{2\pi}_{\Lambda NN}$ for light HN can be only mildly repulsive or even attractive.

In an earlier version of our approach to the SP energies [11], the contribution of $V^{2\pi}_{\Lambda NN}$ to $D(\rho)$ was not adequately calculated, and was repulsive at all ρ and therefore for all HN. A more complete calculation may well give a contribution which is repulsive at larger $\rho \approx \rho_0$ but which becomes less repulsive or even attractive for small ρ; but such a calculation remains to be done. We therefore take a more phenomenological approach which allows for the possibility that the net ΛNN force becomes more repulsive for larger A; this may result from $V^{2\pi}_{\Lambda NN}$ and/or from enhanced suppression of the $\Lambda\Sigma$ coupling for larger ρ with a correspondingly more repulsive $V^D_{\Lambda NN}$. We therefore use only a $V^D_{\Lambda NN}$ of the form of Eq. (6) for which the corresponding correlations are well under control. From now on $V^D_{\Lambda NN}$ is denoted by just $V_{\Lambda NN}$. However, to allow for repulsive contributions which increase with A we include a purely phenomenological density dependent factor for $V_{\Lambda NN}$, namely,

$$F_\beta(\rho) = [1 - \exp(-\beta\rho^2/\rho_0^2)]/[1 - e^{-\beta}] \quad \text{for } \rho < \rho_0 = 1 \text{ for } \rho \leqslant \rho_0. \tag{7}$$

$F_\beta(0) = 0$, where $\beta = \infty$ is equivalent to $F_\beta(\rho) \equiv 1$. The effect of $F_\beta(\rho)$ is to give a less repulsive ΛNN contribution for $\rho < \rho_0$, and since lighter HN have relatively more surface to give a net contribution which becomes more repulsive for larger A. The details of how $F_\beta(\rho)$ is used is given in Sec. III; the relation between $F_\beta(\rho)$ and an equivalent A dependence of W is discussed in Sec. V.

III. CALCULATION OF THE Λ SINGLE-PARTICLE ENERGIES

The B_Λ are obtained from a Schrödinger equation with the potential U_Λ and with an effective mass m^*_Λ:

$$\left[-\frac{\hbar^2}{2m^*_\Lambda(r)} \frac{d^2}{dr^2} + \frac{\hbar^2 l_\Lambda(l_\Lambda+1)}{r^2} + U_\Lambda(r) \right] \Phi_{l_\Lambda} = -B_\Lambda \Phi_\Lambda . \tag{8}$$

The calculation of U_Λ and m^*_Λ is described below. Here we characterize the theoretical status and reliability of these calculations.

The variational calculations for D, which is the Λ binding to nuclear matter, use the wave functions (10) to (12) implemented through the Fermi-hypernetted-chain technique. For a direct ΛN potential ($\epsilon = 0$), the corresponding (local) SP potential is then obtained by folding the effective interaction given by Eq. (16) into the density distribution $\rho(r)$ of the core nucleus to give $U^d_\Lambda(r)$ [Eq. (35)]. For a short-range correlation factor $f_{\Lambda N}(r)$ the corresponding well depth $D^{\Lambda N}_0$ is then very nearly proportional to ρ, and $U^d_\Lambda(r)$ then very nearly corresponds to the use of the lowest-order cluster expansion which, as we shall show, is a good approximation. This folding procedure then corresponds quite closely to a Brueckner-Hartree calculation for hypernuclei. For a $V_{\Lambda NN}$ given by Eq. (6) the corresponding effective potential is given by Eq. (29) and for a short-range $f_{\Lambda N}$ to a good approximation by Eq. (34); the depth $D^{\Lambda NN}$ [Eq. (26)] is then very nearly proportional to ρ^2, with the corresponding $U^{\Lambda NN}_\Lambda$ [Eq. (37)] obtained by double folding of the effective interaction Eqs. (30) and (34). Thus for a direct $V_{\Lambda N}$ plus a dispersive $V_{\Lambda NN}$ our folding procedure should be an excellent approximation.

The Λ binding $D(\rho, k_\Lambda)$ for nuclear matter of density ρ and for a Λ momentum k_Λ is calculated with the FHNC method [3,7]. Thus for $A \to \infty$,

$$-D(\rho,k_\Lambda) = \frac{\langle \Psi^{(A)} | H^{(A)} | \Psi^{(A)} \rangle}{\langle \Psi^{(A)}, \Psi^{(A)} \rangle} - \frac{\langle \Psi^{(A-1)} | H^{(A-1)}_N | \Psi^{(A-1)} \rangle}{\langle \Omega^{(A-1)}, \Psi^{(A-1)} \rangle}, \tag{9}$$

where $H^{(A)}$, $\Psi^{(A)}$ are the Hamiltonian and wave function of the hypernucleus and $H^{(A-1)}_N$, $\Psi^{(A-1)}$ those of the core nucleus. The variational wave functions are

$$\Psi^{(A)} = e^{i\vec{k}\cdot\vec{r}_\Lambda} F \Psi^{(A-1)}, \tag{10}$$

with

$$F = \left[\prod_{i=1}^{A-1} f_{\Lambda N}(r_{\Lambda i}) \prod_{i<j}^{A-1} f_{\Lambda NN}(\vec{r}_{\Lambda i}, \vec{r}_{\Lambda j}, \vec{r}_{ij}) \right] \tag{11}$$

and

$$\Psi^{(A-1)} = \prod_{i<j}^{A-1} f_{NN}(r_{ij}) \Phi^{(A-1)}(1,2,...,A-1), \tag{12}$$

where $\Phi^{(A-1)}$ is the uncorrelated Fermi gas wave function for nuclear matter of density ρ. Details of the correlation factors $f_{\Lambda N}$, f_{NN}, $f_{\Lambda NN}$ and calculational methods are given in Refs. [3,7]. It should be noted that in all earlier as well as in the present calculations $f_{\Lambda NN}$ was found to be 1 within the errors of the calculations.

The effective mass $m^*_\Lambda(\rho)$ is obtained from a quadratic fit in k_Λ to $D(\rho,k_\Lambda) - D(\rho,k_\Lambda = 0)$ or equivalently from Eq. (23) together with Eq. (21). This procedure for incorporating m^*_Λ into Eq. (8) is equivalent to that of Millener *et al.* [13] who use an equivalent energy-dependent potential.

The well depth can be written as

$$D(\rho,k_\Lambda) = -\frac{\hbar^2 k^2_\Lambda}{2m_\Lambda} + D^{\Lambda N}_0(\rho) + D^{\Lambda N}_x(\rho,k_\Lambda) + D^{\Lambda NN}(\rho), \tag{13}$$

where $D^{\Lambda N}_0$, $D^{\Lambda N}_x$, and $D^{\Lambda NN}$ are the direct ΛN, the exchange ΛN, and the three-body ΛNN contributions, respectively. We define

$$D(\rho) = D(\rho, k_\Lambda = 0) \quad \text{and} \quad D^{\Lambda N}_x(\rho) = D^{\Lambda N}_x(\rho, k_\Lambda = 0). \tag{14}$$

The direct contribution is

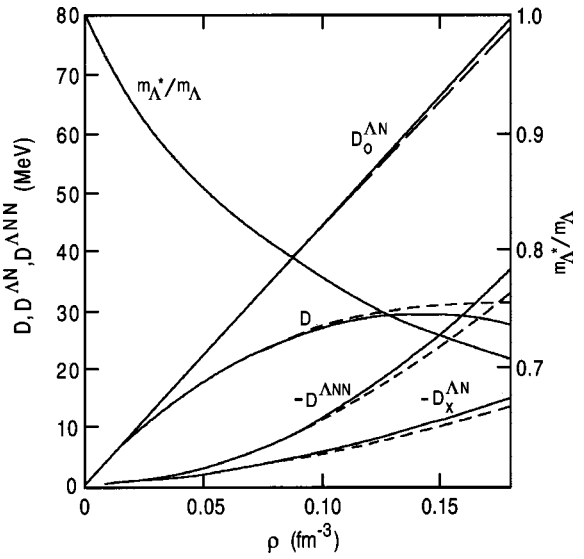

FIG. 3. The well depth D and its components: the direct $D_0^{\Lambda N}$, the exchange $D_x^{\Lambda N}$, and the three-body $D^{\Lambda NN}$ contributions vs the nuclear matter density ρ for the ''exact'' FHNC calculation (full lines) and with the approximation of Eq. (31) (dashed lines) for $V_0=6.2$ MeV, $W=0.02$ MeV, $F_\beta\equiv 1(\beta=\infty)$, and $\epsilon=0.35$. The differences between the ''exact'' and approximate values of m_Λ^*/m_Λ are less than 0.04%.

$$D_0^{\Lambda N}\equiv D^{\Lambda N}(\epsilon=0)=-\langle V\rangle+\langle T_{\Lambda N}\rangle=-\rho\int \tilde{V}_{\Lambda N}d\vec{r}. \tag{15}$$

The effective interaction corresponding to the direct contribution is

$$\tilde{V}_{\Lambda N}=g_{\Lambda N}\left[V_{\Lambda N}(r)-\frac{\hbar^2}{4\mu_{\Lambda N}}\nabla_\Lambda^2\ln f_{\Lambda N}(r)\right], \tag{16}$$

where $\mu_{\Lambda N}$ is the ΛN reduced mass and $g_{\Lambda N}$ is the ΛN distribution function obtained in the FHNC approximation. For a reasonable $V(r)$, $D_0^{\Lambda N}/\rho$ changes by $\lesssim 2\%$ over the range $\rho\lesssim 0.20\,\mathrm{fm}^{-3}$ (Fig. 3).

The ΛN exchange contribution is

$$D_x^{\Lambda N}(\rho,k_\Lambda)=\epsilon\Delta(\rho,k_\Lambda), \tag{17}$$

where

$$\Delta(\rho,k_\Lambda)=\rho\int V_{\Lambda N}(r)\left[g_{\Lambda d}(r)D_F(k_Fr)j_0(k_\Lambda r)-g_{\Lambda N}\right]d\vec{r} \tag{18}$$

is independent of ϵ, k_F is the Fermi momentum, and

$$D_F(x)=\frac{3j_i(x)}{x}=1-\frac{x^2}{10}+\cdots. \tag{19}$$

j_0 and j_1 are the zeroth and first order spherical Bessel functions and $g_{\Lambda N}$, $g_{\Lambda d}$, etc., are defined in Ref. [3]. For small k_Λ we keep only terms in k_Λ^2 in the expansion of j_0 in powers of $k_\Lambda r$; then

$$D_x^{\Lambda N}(\rho,k_\Lambda)=\epsilon[\Delta(\rho,k_\Lambda=0)-\rho bk_\Lambda^2], \tag{20}$$

with

$$b=\frac{1}{6}\int V_{\Lambda N}g_{\Lambda d}D_F(k_Fr)r^2d\vec{r}. \tag{21}$$

Combining the term proportional to k_Λ^2 in Eq. (20) with Eq. (13) we obtain

$$D(\rho,k_\Lambda)=-\frac{\hbar^2k_\Lambda^2}{2m_\Lambda^*}+D(\rho), \tag{22}$$

where

$$\frac{\hbar^2k_\Lambda^2}{2m_\Lambda^*}=\frac{\hbar^2k_\Lambda^2}{2m_\Lambda}-\epsilon\rho bk_\Lambda^2 \tag{23}$$

or, equivalently,

$$\chi\equiv\frac{m_\Lambda}{m_\Lambda^*}-1=-\frac{2m_\Lambda}{\hbar^2}\epsilon\rho b. \tag{24}$$

The effective interaction corresponding to $D_x^{\Lambda N}$ is

$$\tilde{V}_{\Lambda N}^x=\epsilon V_{\Lambda N}(r)[g_{\Lambda d}(r)D_F(k_Fr)-g_{\Lambda N}]. \tag{25}$$

For the dispersive ΛNN interaction, Eq. (6), the ΛNN contribution is

$$D^{\Lambda NN}(\rho)=\frac{1}{2}W\rho^2\int T_\pi^2(r_{\Lambda 1})T_\pi^2(r_{\Lambda 2})g_3(r_{\Lambda 1},\rho_{\Lambda 2},r_{12})d\vec{r}_1d\vec{r}_2d\vec{r}_\Lambda, \tag{26}$$

with

$$g_3=\sum_{x,x',y,y'}g_{xx'}(r_{12})g_{\Lambda y}(r_{\Lambda 1})g_{\Lambda y'}(r_{\Lambda 2}), \tag{27}$$

where x, x', y, and y' represent all the possible exchange patterns consistent with the Pauli exclusion principle (Ref. [3]). For a short-range ΛN correlation factor $f_{\Lambda N}$ the dominant ρ variation of $D^{\Lambda NN}$ comes from the ρ^2 term in Eq. (26). With the density modification of Eq. (7),

$$D_\beta^{\Lambda NN}(\rho)=F_\beta(\rho)D^{\Lambda NN}(\rho). \tag{28}$$

We define an effective ΛNN interaction

$$\tilde{V}_{\Lambda NN}=W_0T_\pi^2(r_{\Lambda 1})T_\pi^2(r_{\Lambda 2})g_3 \tag{29}$$

and with the density modification

$$\tilde{V}_{\Lambda NN}^{(\beta)}=F_\beta(\rho)\tilde{V}_{\Lambda NN}. \tag{30}$$

In the following, the index β is mostly implied and omitted.

For the calculation of $U_\Lambda(r)$ the use of the effective interactions $\tilde{V}_{\Lambda N}$, $\tilde{V}_{\Lambda N}^x$, and $\tilde{V}_{\Lambda NN}$ includes the density depen-

dence arising from the density dependent correlations. However, for a short-range ΛN correlation, this dependence is quite weak. In this case the approximation

$$g_{\Lambda N}, g_{\Lambda d} \approx f_{\Lambda N}^2, g_{NN} \approx f_{NN}^2 \approx 1 \tag{31}$$

is then very good for the calculation of $D_0^{\Lambda N}$, $D_x^{\Lambda N}$, and $D^{\Lambda NN}$, and m_Λ^* and, therefore, also of $D(\rho)$. With Eq. (31) our effective interactions become

$$\tilde{V}_{\Lambda N} = f_{\Lambda N}^2 \left[V_{\Lambda N}(r) - \frac{\hbar^2}{4\mu_{\Lambda N}} \nabla_\Lambda^2 \ln f_{\Lambda N}(r) \right], \tag{32}$$

$$\tilde{V}_{\Lambda N}^x = \epsilon f_{\Lambda N}^2 V_{\Lambda N}(r)[D_F(k_F r) - 1], \tag{33}$$

$$\tilde{V}_{\Lambda NN} = W_0 f_{\Lambda 1}^2(r_{\Lambda 1}) f_{\Lambda 2}^2(r_{\Lambda 2}) T_\pi^2(r_{\Lambda 1}) T_\pi^2(r_{\Lambda 2}). \tag{34}$$

In Fig. 3 the solid curves depict the results of an ''exact'' FHNC calculations using Eqs. (16), (25), and (26). The dashed curve gives the results of a calculation using the approximations (32)–(34). The small differences between the two sets of curves shows that Eq. (31) is a very good approximation; the differences in m_Λ^* are less than 0.04%.

We remark that the use of the ''exact'' FHNC method (exact except for the negligible elementary diagrams) is essential to preserve the variational nature of the calculation of D. A free variation of $f_{\Lambda N}$ using Eq. (31) will not give a lower bound to D. Thus $f_{\Lambda N}$ as used in the lowest order cluster approximation must be constrained by the use of a complete FHNC calculation.

For the calculation of $U_\Lambda(r)$ we fold the effective interactions (32)–(34) with the nuclear density $\rho(r)$:

$$U_\Lambda^d(r) = (A-1) \int a_d(\rho) \tilde{V}_{\Lambda N}(|\vec{r} - \vec{r}'|) \rho(r') d\vec{r}', \tag{35}$$

$$U_\Lambda^x(r) = (A-1) \int a_x(\rho) \tilde{V}_{\Lambda N}^x(|\vec{r} - \vec{r}'|) \rho(r') d\vec{r}', \tag{36}$$

$$U_\Lambda^{\Lambda NN}(r) = \frac{1}{2}(A-1)(A-2) \int a_{\Lambda NN}(\rho) \tilde{V}_{\Lambda NN}^{(\beta)} \times (|\vec{r} - \vec{r}'|, |\vec{r} - \vec{r}''|) \rho(r') \rho(r'') d\vec{r}' d\vec{r}'', \tag{37}$$

$$U_\Lambda(r) = U_\Lambda^d(r) + U_\Lambda^x(r) + U_\Lambda^{\Lambda NN}(r). \tag{38}$$

In the above expressions the density-dependent factors $a_d(\rho)$, $a_x(\rho)$, and $a_{\Lambda NN}(\rho)$ are chosen such that the effective interactions (32)–(34) reproduce the ''exact'' FHNC results (corresponding to the solid curves of Fig. 3). These correction factors are mostly quite close to unity. In this way we compensate for the errors we may have introduced through Eq. (31) in the calculation of $U_\Lambda(r)$. The density-dependent factor $F_\beta(\rho)$ is of course purely phenomenological.

We briefly discuss finite-range effects for $D_x^{\Lambda N}$ and m_Λ^*. A zero-range force is equivalent to retaining terms up to x^2 in Eq. (19) for $D_F(x)$. Then

$$(\Delta_0/\rho^{5/3}) = -\frac{3}{5}\left(\frac{3\pi^2}{2}\right)^{2/3} b_0, \tag{39}$$

where Δ_0 denotes $\Delta(\rho, k_\Lambda = 0)$ in the zero-range limit and

$$b_0 = b(\rho = 0) = \frac{1}{6} \int V_{\Lambda N} g_{\Lambda N} r^2 d\vec{r}. \tag{40}$$

Then

$$\Delta(\rho, k_\Lambda = 0) = \Delta_0 F_1, \tag{41}$$

with

$$F_1 = \Delta(\rho, k_\Lambda = 0)/\Delta_0. \tag{42}$$

Similarly for m_Λ^* we have

$$\chi \equiv \frac{m_\Lambda}{m_\Lambda^*} - 1 = -\frac{2m_\Lambda}{\hbar^2} \epsilon \rho b_0 F_2, \tag{43}$$

with

$$F_2 = b/b_0. \tag{44}$$

$F_1(\rho)$, $F_2(\rho)$ are form factors which represent finite range effects of $V_{\Lambda N}$. The Hartree-Fock expressions are obtained by putting $g_{\Lambda N} = 1$. (For a Yukawa potential $\sim \exp(-\mu r)/r$ the HF form factors are $F_1 = 2.5\alpha^{-2}[1 - 3\alpha^{-3}(\alpha - \tan^{-1}\alpha)]$, $F_2 = (1+\alpha^2)^{-2}$, where $\alpha = \mu^{-1} k_F$.) Finite-range effects ($F_1, F_2 < 1$) are more important for χ, i.e., for m_Λ^*, than for Δ: $F_1 \approx 0.8$, $F_2 \approx 0.5$ at ρ_0 and $F_1 \simeq 0.9$, $F_2 \simeq 0.7$ at $0.5\rho_0$. Thus, the ρ dependence of $D_x^{\Lambda N}$ is close to proportional to $\rho^{5/3}$, as for a zero-range force. The ratio $D_x^{\Lambda N}/\chi \sim \rho^{2/3} F_1/F_2$ is a function only of ρ and differs from that for a Skyrme force ($F_1 \equiv F_2 \equiv 1$) used by Millener *et al.* [13]. Comparison with the form factors for a Yukawa potential shows that $\mu \approx 1.1\ \mathrm{fm}^{-1}$ gives a fair fit to F_1 and $\mu \approx 2\ \mathrm{fm}^{-1}$ a surprisingly good fit to F_2. There is, of course, no reason to expect a particularly good fit with a Yukawa shape or that μ should be the same for F_1 and F_2.

The expressions for the s- and p-state contributions to the total ΛN depth are

$$D^{\Lambda N} = D_0^{\Lambda N} + D_x^{\Lambda N} \simeq D_s + D_p, \tag{45}$$

where we have neglected the small ($\simeq 1.5$ MeV) d-state contribution. Thus using Eqs. (1) and (4),

$$D_s = D_0^{\Lambda N} + \frac{\Delta}{2}, \quad D_p = -(1 - 2\epsilon)\frac{\Delta}{2}, \tag{46}$$

where $\Delta = D_x^{\Lambda N}/\epsilon$ is independent of ϵ. We note that D_p, $V_p = 0$ for $\epsilon = 0.5$ and that $D_p < 0$ for $\epsilon > 0.5$, corresponding to a repulsive V_p.

TABLE II. Calculated B_Λ and χ_l^2 for selected fits. The top row gives V_0, W, β, ϵ for each fit. The B_Λ are shown for each l value. The value in parentheses for $^{13}_{\Lambda}$C is the χ^2 (per B_Λ) for all five $_\Lambda$C states. The bottom row shows the χ_l^2 (per B_Λ); the value in parentheses is χ_d^2 (per B_Λ) omitting ^{40}Ca(d). All energies are in MeV.

	NO FF				WITH FF															
	6.2, s	0.02, p	∞, d	0.35 f	6.2, s	.028, p	∞, d	0 f	6.2, s	.024, p	∞, d	0.11 f	6.2, s	.021, p	2.0, d	0.255 f	6.15, s	.020, p	2.0, d	0.22 f	6.1, s	0.02, p	0.1, d	0.20 f
$^{11}_{\Lambda}$C	10.4				9.1				8.7				9.1				8.8				8.9			
$^{12}_{\Lambda}$C	10.9	−0.4			9.7	1.0			9.4	0.5			9.5	0.3			9.3	0.3			9.2	0.2		
$^{13}_{\Lambda}$C	11.5	0.1	(0.6)		10.4	1.6	(4.6)		10.1	1.0	(5.6)		10.2	0.9	(4.1)		10.0	0.8	(6.0)		10.0	0.8	(5.7)	
$^{16}_{\Lambda}$O	13.3	1.9			12.1	3.4			11.9	2.6			12.3	2.5			12.0	2.4			12.3	2.5		
$^{28}_{\Lambda}$Si	16.9	6.9			15.8	8.2			16.0	7.5			16.1	7.4			15.9	7.3			15.8	7.5		
$^{32}_{\Lambda}$S	17.6	8.2			16.6	9.4			16.8	8.7			16.8	8.6			16.7	8.5			16.4	8.8		
$^{40}_{\Lambda}$Ca	19.0	10.3	1.4		18.2	11.3	4.0		18.6	10.7	3.0		18.9	10.9	2.8		18.8	10.8	2.7		19.0	11.2	3.1	
$^{51}_{\Lambda}$V	20.0	11.9	3.2		19.2	12.8	6.0		20.1	12.5	5.0		19.6	12.1	4.6		19.7	12.1	4.6		19.0	12.1	4.8	
$^{89}_{\Lambda}$Y	22.1	15.9	8.8	1.4	21.6	16.5	11.0	4.9	22.8	16.8	10.4	3.8	22.1	16.2	9.9	3.3	22.3	16.3	10.0	3.3	21.0	16.0	10.1	3.6
$^{139}_{\Lambda}$La	23.8	18.9	13.0	6.5	23.8	19.5	14.6	9.5	25.2	20.1	14.6	8.7	24.8	19.7	14.1	8.2	25.0	19.9	14.2	8.2	24.4	19.7	14.5	8.7
$^{208}_{\Lambda}$Pb	24.9	21.0	16.2	10.7	25.4	21.6	17.5	13.1	26.9	22.6	17.9	12.9	26.9	22.5	17.6	12.5	27.0	22.6	17.7	12.6	26.9	22.5	17.9	12.9
χ_l^2	2.2	1.0	0.6(0.5)	1.3	2.5	1.8	14.0(3.0)	5.9	3.2	0.7	5.8(1.0)	1.7	2.2	0.5	4.4(0.2)	0.6	3.3	0.5	4.2(0.3)	0.7	3.3	0.5	5.9(0.5)	1.2

IV. FITS TO THE SP ENERGIES

A. Parameters and inputs to fits of SP energies

Potential parameters. The B_Λ are obtained from Eq. (8), with $U_\Lambda(r)$ and $m_\Lambda^*(r)$ calculated for a given set of potential parameters as described in Sec. III. In our fits we use the ΛN strength $V_0 = 6.15 \pm 0.5$ MeV as constrained by the scattering data. The strength W of the ΛNN potential is allowed to vary within wide limits (0–0.04 MeV). The parameter β in $F_\beta(\rho)$, which modifies the ΛNN potential in the surface, is allowed to vary from 0.1–∞, where ∞ corresponds to $F_\infty(\rho) \equiv 1$, i.e., to the unmodified ΛNN interaction of Eq. (6). The exchange fraction ϵ is allowed to vary freely since it is so poorly determined by the Λp scattering. The strength $V_0^{\rm CSB}$ of the CSB potential is allowed to vary from -0.1 to 0.1 MeV, which includes $V_0^{\rm CSB} \simeq -0.05$ MeV obtained from the $A=4$ HN. The fits are then determined by five parameters of which V_0 is strongly constrained, and $V_0^{\rm CSB}$, for the values considered, has a minor but significant effect only for the heavy HN. The number of experimental B_Λ to be fitted is 24.

Core-nucleus densities. These are obtained from the compilation of charge densities ρ_c of Ref. [28], using in each case the most accurate fit to the electron-scattering data. To obtain the matter densities ρ, the densities ρ_c were unfolded with the (exponential) proton charge density ρ_p. The use of two different fitted ρ_c (sum of 12 G and a three-parameter Fermi distribution) was considered for $^{40}_{\Lambda}$Ca and made only a very small difference in B_Λ ($\simeq$0.02 MeV). All ρ_c except for $^{13}_{\Lambda}$C are for $A_c = A$ but normalized to $A-1$. For $^{13}_{\Lambda}$C we use $\rho(^{12}\mathrm{C})$.

The experimental B_Λ. These (Refs. [1,2]) are shown in Fig. 1 and in Table I. In order not to give undue weight to the five very accurate $_\Lambda$C energies, we give each of these a nominal error of 0.5 MeV in our fits. We calculate three different χ^2 per degree-of-freedom (B_Λ): χ^2 for all $N=24$, χ_1^2 omitting $^{40}_{\Lambda}$Ca(d) ($N=23$), and χ_2^2 omitting both $^{40}_{\Lambda}$C(d) and all five $_\Lambda$C values ($N=18$) where $_\Lambda$C is a shorthand for the three HN: $^{11}_{\Lambda}B$, $^{12}_{\Lambda}$C, $^{13}_{\Lambda}$C.

All energies V_0, W, B_Λ, D, etc., are in MeV; ρ is in fm^{-3}; $B_\Lambda(s)$,..., refer to the s state, . . . , energies.

The dependence of χ^2 on the potential parameters was systematically explored with and without FF, and is presented in Table III for $V_0 = 6.2$ for which the most complete search was made, and in Table IV for $V_0 = 6.1$; a somewhat less complete search was also made for $V_0 = 6.15$. With CSB, more detailed results are shown in Table IX. For a given V_0 and for each W and β, the optimum value of ϵ together with the corresponding χ^2, χ_1^2, χ_2^2 were obtained. This optimum ϵ is well determined. It is these values which are discussed and shown in the tables. The results for selected fits, including some of our best fits are shown in Table II. Figure 1 also shows one of our best fits (with FF) for $V_0 = 6.2$. Figure 4 shows $D(\rho)$ and its components for several fits, and Fig. 5 shows some selected SP potentials.

B. Fits with only a ΛN potential

Direct ΛN potential. For this $\epsilon = 0$ and hence $m_\Lambda^* = m_\Lambda$. $D(\rho) = D_0^{\Lambda N}(\rho)$ which is to a very good approximation pro-

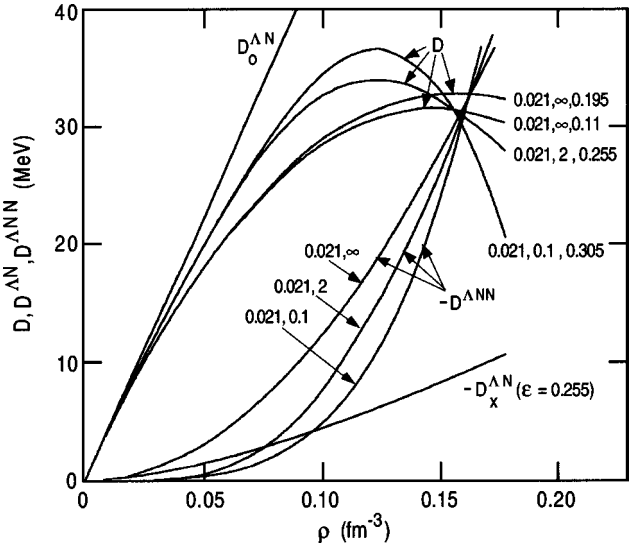

FIG. 4. The well depth and its components vs the nuclear matter density ρ. All results are for $V_0=6.2$ MeV for D; the triplets are the values of W,β,ϵ; for $D^{\Lambda NN}$, the doublets are the values of W,β.

portional to ρ as discussed in Sec. III with $D_0^{\Lambda N}=(420\pm20)\rho$ for $V_0=6.15\pm0.05$. Then $D_\Lambda=D_0^{\Lambda N}(\rho_0)=69\pm3$ MeV and all the B_Λ are much too large. If V_0 were adjusted—without any justification—to give $D_\Lambda\simeq30$ MeV so as to roughly fit the $B_\Lambda(s)$ for large A, then the B_Λ, even for moderate A, would be much too small (and the ΛN cross section also much too small). This conclusion, as already discussed, implies the need for a strongly repulsive contribution at large ρ, in order to give $D_\Lambda\simeq30$ MeV.

ΛN potential with space exchange. For $\epsilon>0$ the exchange contribution is repulsive and could conceivably be such as to give a reasonable fit; for a given V_0 there is now only the one parameter ϵ. For $V_0=6.2$ our best fit with FF is obtained for $\epsilon\approx0.79$ and correspondingly $m_\Lambda^*(\rho_0)=0.53\,m_\Lambda$, with a very large $\chi^2\simeq39$ and with $D_\Lambda\simeq42$ MeV. This effectively demonstrates that it is impossible to find even a tolerable fit for a $V_{\Lambda N}$ with space exchange. Without a FF the fit is even worse: much too small B_Λ for large A; too large spacings between $B_\Lambda(l)$ for different l (m_Λ^* is very small).

Thus a ΛN potential only—with or without exchange—is ruled out by the SP B_Λ data.

C. Effect of fringing field (FF)

For the specific effect of the finite range of the ΛN and ΛNN potentials, i.e., of the FF, we consider the theoretically firmest case: $\epsilon=0$, $\beta=\infty$. This case has the least uncertainties, in particular about the FF: no space exchange ($m_\Lambda^*\equiv m_\Lambda$) implies there are no approximations involving any nonlocality of $V_{\Lambda N}$, and $\beta=\infty$ ($F_\beta\equiv1$) implies the ΛNN potential is given by Eq. (6) without any phenomenological ρ dependence. Thus the only parameter for fixed V_0 is W. Tables III and IV show the dependence of χ^2 on W and Table II the results for the best fits: for $V_0=6.2$, we obtain $W=0.032$ without FF, and $W=0.028$ with FF. The dramatic improvement with a FF [from $\chi^2=10.3$ (no FF), to 3.8 (FF)] is striking and seems strong evidence for its reality. This fit

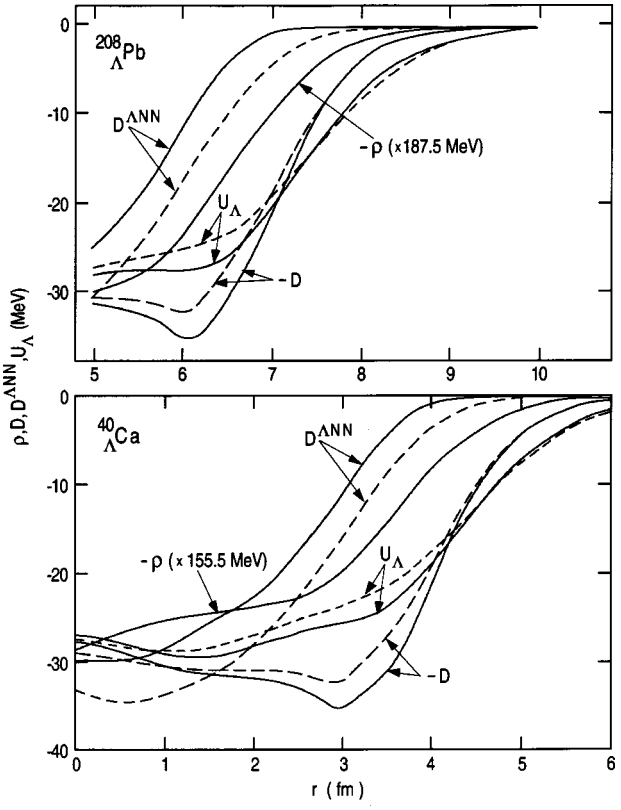

FIG. 5. The Λ-core nucleus potentials for ${}^{40}_{\Lambda}$Ca and ${}^{208}_{\Lambda}$Pb. U_Λ is the potential with FF, $D\equiv D[\rho(r)]$ is the potential without FF, and $U^{\Lambda NN}$ is the ΛNN contribution to U_Λ. The full lines are for $V_0=6.2$ MeV, $W=0.021$ MeV, $\beta=2$, and $\epsilon=0.255$, and the dashed lines are for $V_0=6.2$ MeV, $W=0.024$ MeV, $F_\beta\equiv1$, and $\epsilon=0.11$.

with FF is overall fair; the $B_\Lambda(s)$ are well fitted, but the fits for $l>0$ are poor. The larger W required without FF reflects the need for more repulsion than with FF because the shorter range of the SP potential without FF enhances binding. Thus for a fixed set of parameters (e.g., $V_0=6.2$, $W=0.032$) the effect of a FF is to give a large decrease of B_Λ: about 3–4 MeV for $A\leqslant51$ and about 2 MeV for larger A [for $B_\Lambda(s)$]. Some of our best fit SP potentials with and without FF are shown in Fig. 5 and are discussed further below.

D. Fits without FF

The dependence of the χ^2 on the potential parameters ϵ, W (for $\beta=\infty$) are shown in Tables III and IV. The best fits are obtained for $V_0=6.2$ with $W=0.02$, $\epsilon=0.35$, and for $V=6.1$ with $W=0.02$, $\epsilon=0.22$. These are excellent fits and are shown in Tables III and IV. That for $V_0=6.2$ (slightly better than for $V_0=6.1$) is also shown in more detail in Table II and is close to one we found earlier [11] and is also close to the ρ^2 nonlocal fits of Millener *et al.* with $m_\Lambda^*/m_\Lambda\approx0.8$, $D_\Lambda\approx28$ [13]. The inclusion of recent data for ${}^{139}_{\Lambda}$La and especially for ${}^{208}_{\Lambda}$Pb worsens the fit and shows the importance of data for large A. $F_\beta(\rho)<1$ (i.e., $\beta\neq\infty$) and/or inclusion of a negative CSB worsen the fits, but a rather large positive CSB improves the fits considerable (Sec. VI); also ${}^{40}_{\Lambda}$Ca(d) and $A<13$ are quite well fitted and better than with FF.

TABLE III. χ^2 (per B_Λ) for interactions with $V_0=6.2$ MeV. For each W (MeV) and β the optimum ϵ is shown. The three values of χ^2 are in descending order: χ^2 for all 24 B_Λ, χ^2 omitting ${}^{40}_{\Lambda}\mathrm{Ca}(d)$, χ^2 omitting ${}^{40}_{\Lambda}\mathrm{Ca}(d)$, and all ${}_{\Lambda}\mathrm{C}$. Values in parenthesis are with a CSB potential $V_0^{\mathrm{CSB}}=-0.05$ MeV with FF and 0.1 without FF.

		With FF					No FF		
W(MeV)=		0.028	0.026	0.024	0.021	0.018	0.032	0.026	0.02
β									
∞	$\epsilon=$	0.00	0.06	0.11	0.195	0.28	0.00	0.18	0.35
		3.82	2.86	2.52(2.17)	3.25	5.35	10.26	3.9	1.50(0.89)
		2.43	2.00	1.96(1.59)	3.14	5.54	9.22	3.7	1.54(0.91)
		1.84	1.17	0.94(0.64)	1.87	3.08	10.86	4.6	1.79(0.98)
4	$\epsilon=$	0.05	0.10	0.15	0.23	0.31			
		5.71	3.71	2.46	2.10	3.41			
		3.86	2.34	1.53	1.74	3.44			
		3.82	1.99	0.90	0.72	2.15			
2	$\epsilon=$	0.09	0.13	0.18	0.255	0.33			
		6.32	4.01	2.52	1.77(1.56)	2.78			
		4.36	2.44	1.45	1.30(1.07)	2.73			
		4.65	2.36	1.07	0.50(0.36)	1.66			
0.1	$\epsilon=$	0.16	0.20	0.24	0.305	0.37			
		6.31	4.12	2.57	1.66(1.57)	2.46			
		4.54	2.77	1.61	1.22(1.11)	2.40			
		5.13	2.94	1.42	0.58(0.55)	1.49			

However, as discussed further in Sec. V, these fits are not reconcilable with ${}^{5}_{\Lambda}\mathrm{He}$ which requires a much smaller $W\approx 0.01$.

We also made calculations for the same parameters ($V_0=6.2$, $W=0.02$, $\epsilon=0.35$) but using the charge distribution ρ_c instead of ρ. This gives a very small decrease of $\lesssim 0.1$ MeV in the B_Λ even for smaller A where the difference is largest. Thus the proton charge distribution is quite inadequate in representing the effect of a realistic FF inspite of its rms radius of 0.8 fm (also Ref. [14]).

Although a FF field gives a dramatically improved fit in the absence of exchange, the dependence on the exchange fraction ϵ and also on W is considerably greater without than with a FF (presumably because the SP potentials extend further with a FF), leading without FF to a steeper descent in the $\chi^2(\epsilon,W)$ surface, which is then responsible for the somewhat better fits without FF when ϵ is switched on. We again emphasize that the FF is demanded by the physics and that a fit without FF, however good, is difficult to justify.

E. Fits with FF

Systematic searches were made for $V_0=6.1$, 6.15, and most completely for 6.2, providing the complete landscape of the dependence of the χ^2's on the potential parameters. Different fits can be comparable because considerable compensation can occur: decreasing V_0 and increasing W, β, ϵ all correspond to more repulsion. In particular, ϵ (whose effect occurs both through the potential and m^*_Λ) is not very precisely determined. Nevertheless, as seen from Tables III and IV, a region of minimum $\chi^2\lesssim 2$ (for $V_0=6.2$) is quite well determined. We discuss mostly the fits for $V_0=6.2$, since the considerations for $V_0=6.1$ and 6.15 are quite similar.

The fit for $\epsilon=0$ and $\beta=\infty$ (upper left hand of Table III) was already discussed. For given β the best fit occurs for some intermediate value of W in the range shown; the optimum ϵ increases as W decreases as a result of the compensation just discussed. In particular, we note that the rather good fit obtained for $\beta=\infty$ with $W=0.024$, $\epsilon=0.11$ which is also shown in Table II. Thus if no modification of the ΛNN contribution arising from $F_\beta(\rho)<1$ had been made, this fit would have been considered the best with FF: it is in fact quite good and not much poorer than the best fits to be discussed below. Again as without FF, this fit, apart from not being the best if β is allowed to vary, is not reconcilable with ${}^{5}_{\Lambda}\mathrm{He}$, which requires $W\simeq 0.01$.

For a given W the best fits with FF occur for smaller $\beta\simeq 0.1-2$, with the optimum ϵ increasing as β decreases: the exchange contribution becomes more repulsive for larger ϵ whereas the ΛNN contribution becomes less repulsive for small β since this implies a less repulsive ΛNN contribution from the surface. There is then a valley of minimum χ^2 running diagonally from the upper left (large W,β) to the lower right (small W,β) with the lowest values occurring for $\beta\simeq 0.1-2$, $W\simeq 0.021$ and correspondingly $\epsilon\simeq 0.25-0.30$. This region of minimum $\chi^2\lesssim 2$ is quite well determined. If ${}^{40}_{\Lambda}\mathrm{Ca}(d)$ is omitted, a significantly smaller $\chi^2_1\lesssim 1.3$ is obtained, the parameters of the corresponding best fit region changing only very slightly. The further omission of the ${}_{\Lambda}\mathrm{C}$ values give the best values as $\chi^2_2\lesssim 0.6$ and changes the best fit region to somewhat larger β (for both $V_0=6.2$ and 6.1). This is because the $A>13$ HN (which dominate χ^2 and χ^2_1)

TABLE IV. χ^2 (per B_Λ) for interactions with $V_0=6.1$ MeV and for best fit interactions with $V_0=6.15$ MeV. As for Table III, values are with FF except for last column without FF.

W(MeV)=	0.024	0.022	0.020	0.018	0.02
β					
∞	ϵ=	0.04		0.15	0.23
		4.00		5.67	1.68
		3.49		5.70	1.65
		1.72		3.81	1.98
4	ϵ=	0.07	0.13	0.18	
		3.38	3.29	3.87	
		2.39	2.82	3.70	
		1.26	1.24	2.02	
2	ϵ= 0.05	0.10	0.15	0.20	
	4.33	3.14	2.80	3.26	
	2.71	2.06	2.21	3.04	
	2.16	1.14	1.02	1.55	
0.1	ϵ=	0.15	0.20	0.24	
		2.96	2.50(2.29)	2.82	
		1.84	1.87(1.64)	2.48	
		1.22	0.80(0.67)	1.31	
	Best fit interactions for $V_0=6.15$ MeV				
	$W=0.020$ MeV				
2	ϵ= 0.22				
	2.27(1.96)				
	1.84(1.50)				
	0.70(0.44)				
0.1	ϵ= 0.26				
	2.04(1.79)				
	1.53(1.25)				
	0.75(0.53)				

prefer a value of β which gives too small B_Λ for $_\Lambda$C. Further related discussion is in Sec. V.

The $^{40}_{\Lambda}$Ca(d) value does not fit the pattern of $B_\Lambda(d)$ values for any of our fits *with FF*. Our best fits with FF all give $B_\Lambda \simeq 3$ MeV for $^{40}_{\Lambda}$Ca(d) as compared with the experimental $B_\Lambda \simeq 1$ MeV. This suggests that the experimental B_Λ should be confirmed. It is difficult to see how structure effects could be large enough to account for the difference. Conceivably, the Λ in a d state could act as a pseudoneutron, closing the s-d shell; but this would be expected to give more binding and is thus in the wrong direction to account for the experimental energy. In any case, omitting $^{40}_{\Lambda}$Ca(d) does not change the best-fit parameters. We recall that our best fits without FF (Table II) give $B_\Lambda \approx 1.5$ MeV for $^{40}_{\Lambda}$Ca(d) as well as values for $_\Lambda$C in good agreement with experiment. If we do not rule out this fit on the grounds of a theoretical need for a FF and of consistency with $^{5}_{\Lambda}$He then a definitive determination of B_Λ for $^{40}_{\Lambda}$Ca(d) becomes critical.

The best fits with FF, apart from $^{40}_{\Lambda}$Ca(d) and $_\Lambda$C, are very good and reproduce the experimental B_Λ very well. The inclusion of a reasonable negative CSB potential consistent with $A=4$ improves the fits with FF for large A even further, whereas our best fits without FF are worsened; however, the latter are considerably improved with a rather large *positive* CSB potential. Our best fits (shown in Table II) do not differ too much in their B_Λ values. For $V_0=6.1$ and 6.15 (Table IV) the pattern of fits is quite similar to that for $V_0=6.2$. Although the best fits are quite good, they are somewhat inferior to those for $V_0=6.2$. Because $V_{\Lambda N}$ is now less attractive, the best fits occur for slightly smaller $W \simeq 0.02$ and correspondingly smaller $\epsilon \simeq 0.23$. The best fits are for $\beta=0.1$; these are slightly better than for $\beta=2$, and both give very similar B_Λ.

F. Best-fit parameters and other quantities

Some fits including our best (marked with *) together with the associated well depth $D_\Lambda = D(\rho_0)$ and its components, as well as $m^*_\Lambda(\rho_0)/m_\Lambda$ are shown in Table V. If with FF all $V_0=6.15\pm0.05$, consistent with ΛN scattering, are considered equally acceptable, then $\epsilon \simeq 0.2-0.3$, $W=0.02-0.021$, correspondingly, $m^*_\Lambda(\rho_0)/m_\Lambda \simeq 0.75-0.82$ and $V_p/V_s \simeq 0.4-0.6$. Our results suggest that $V_0=6.2$ is preferred, in which case $W \simeq 0.021$, $\beta \simeq 0.1-2$ with $\epsilon \simeq 0.25-0.3$ now being somewhat more precisely determined and correspondingly $m^*_\Lambda(\rho_0)/m_\Lambda \simeq 0.74-0.78$ and $V_p/V_s \simeq 0.4-0.5$. Our best fits without FF (for $V_0=6.1-6.2$) give $W=0.02$, $\epsilon=0.25-0.35$ and $m^*_\Lambda/m_\Lambda=0.72-0.8$, V_p/V_s

TABLE V. Well depth, effective mass, and related quantities. All fits are with FF except where indicated. Our best fits are marked with asterisks. All energies in MeV, ρ in fm^{-3}.

				Values for $\rho_0=0.165$									
V_0	W	β	ϵ	D_Λ	$D_0^{\Lambda N}$	$-D_x^{\Lambda N}$	$-D^{\Lambda NN}$	D_s	D_p	$D_s+D^{\Lambda NN}$	m_Λ^*/m	$D_{\max}$	$\rho_{\max}$
6.2	0.028	∞	0	29.0	72.5	0	43.5	54.1	18.4	10.6	1	30.0	0.140
6.2	0.026	∞	0.06	29.9	72.5	2.2	40.4	54.1	16.2	13.7	0.94	30.6	0.142
6.2	0.24	∞	0.11	31.2	72.5	4.0	37.3	54.1	14.4	16.8	0.89	31.5	0.148
6.2	0.022	2	0.23	29.8	72.5	8.5	34.3	54.1	9.9	19.8	0.79	33.8	0.122
6.2*	0.021	2	0.255	30.4	72.5	8.4	32.7	54.1	10.1	21.4	0.79	33.9	0.124
6.2*	0.021	0.1	0.305	28.4	72.5	11.2	32.7	54.1	7.2	21.4	0.74	36.5	0.126
6.15*	0.02	2	0.22	29.1	69.5	7.9	32.5	51.5	10.1	19.0	0.80	32.7	0.124
6.15	0.02	0.1	0.26	27.5	69.5	9.4	32.5	51.5	8.6	19.0	0.78	35.5	0.126
6.1	0.022	0.1	0.15	27.4	66.5	5.3	33.9	48.7	12.4	14.8	0.86	35.5	0.126
6.1*	0.020	0.1	0.20	28.7	66.5	7.1	30.8	48.7	10.6	17.9	0.82	35.4	0.128
6.1	0.018	0.1	0.24	30.3	66.5	8.5	27.7	48.7	9.2	21.0	0.79	35.6	0.131
No FF													
6.2	0.032	∞	0	22.8	72.5	0	49.8	54.1	18.4	4.3	1	26.3	0.119
6.2*	0.02	∞	0.35	28.6	72.5	12.7	31.1	54.1	5.5	17.6	0.72	29.0	0.144
6.1*	0.02	∞	0.23	27.8	66.5	8.1	30.6	48.7	9.5	18.1	0.80	28.1	0.15

$=0.3-0.5$. The well depth D_Λ is quite similar for all fits with and without FF and is quite well determined independently of V_0: the best fits for $V_0=6.2$ give $D_\Lambda\simeq 28.5-30.5$ and for $V_0=6.1$ and 6.15 give $D_\Lambda\simeq 28-29$.

A new feature of our work is that $F_\beta(\rho)<1$ is required with FF. Our best fits for $\beta=0.1-2$ correspond to a reduced repulsive ΛNN contribution from the surface. Since the surface is relatively more important for small A, this implies an effectively less repulsive ΛNN potential for smaller A. This aspect of our fits is discussed in more detail in Sec. V.

Some results for $D(\rho)$ and its components are shown in Fig. 4 for $V_0=6.2$. In Table V we also show the maximum values $D_{\max}$ and the corresponding densities $\rho_{\max}$. The salient ''saturation'' feature of $D(\rho)$, i.e., a maximum at $\rho_{\max}<\rho_0$, is required by all fits and reflects the competition between the attractive ΛN contribution $D_0^{\Lambda N}$ and the repulsive ΛNN contribution $D^{\Lambda NN}$ with some help from $D_x^{\Lambda N}$. This saturation feature was already clearly pointed out by Millener *et al.* [13] and was also found in our earlier work [11]. The effect of $\beta<\infty$ is quite striking: for smaller β in particular $\beta=2$ and especially $\beta=0.1$, $D(\rho)$ has a larger maximum value and is more sharply peaked than for $\beta=\infty$; the maximum occurs at $\rho_{\max}\simeq 0.125$ for $\beta=0.1$ and 2 and at somewhat lower values $\simeq 0.145$ for $\beta=\infty$ both with and without FF. Figure 4 also clearly shows how for smaller β the ΛNN depth $D^{\Lambda NN}(\rho)$ is smaller corresponding to a lessened repulsive contribution from the surface. The exchange contribution $D_x^{\Lambda N}$ is proportional to ϵ, for a given ρ and V_0, consistent with Eq. (3.14).

Table V also shows the s- and p-state depths D_s and D_p given by Eq. (46), as well as $D_s+D^{\Lambda NN}$ which corresponds to the even-state contribution in G-matrix calculations which include the $\Lambda N-\Sigma N$, $^3S-{}^3D$ contribution whose suppression in nuclear matter is roughly equivalent to a dispersive $V_{\Lambda NN}$. The total well depth is then $D_\Lambda=(D_s+D^{\Lambda NN})+D_p$. We note that our best-fit interactions give $D_s+D^{\Lambda NN}\simeq 18-21$ MeV, whereas the even-state G-matrix contributions are $\simeq 30$ MeV [16,17]; this suggests that the latter are missing about 10 MeV repulsion (see Sec. VII for further discussion).

The sp potentials are shown in Fig. 5 for $^{40}_{\Lambda}$Ca and $^{208}_{\Lambda}$Pb. The potential without FF (i.e., zero-range ΛN force) is just $D[\rho(r)]$. This shows the structure corresponding to $D(\rho)$ in Fig. 4, in particular a minimum: $-D_{\max}$ at a value of r corresponding to $\rho_{\max}$. However, for U_Λ this structure is smoothed out by the finite ΛN range. As already pointed out in Ref. [13], $r_{0.5}(D)\simeq r_{0.5}(\rho)+0.55$ fm because of the nonlinear (with ρ) contributions of $D^{\Lambda NN}$ and to a lesser extent of $D_x^{\Lambda N}$ ($D_0^{\Lambda N}\sim\rho$ to a very good approximation). The $\frac{1}{2}$-value radii of $D[\rho(r)]$ and of $U_\Lambda(r)$ are quite close for all nuclei: $r_{0.5}(U_\Lambda)\simeq r_{0.5}(D)+0.1$ fm. Although $r_{0.5}$ is approximately the same with and without FF, the FF spreads out the sp potentials. Thus defining $\Delta r=r_{0.9}-r_{0.1}$ we obtain $\Delta r(D)\simeq 1.5-1.7$ fm for $\beta=\infty$ and $\simeq 1.3-1.5$ fm for $\beta=2$ whereas $\Delta r(U_\Lambda)\simeq 3.3-3.9$ fm for $\beta=\infty$ and $\simeq 2.0-3.0$ fm for $\beta=2$. As expected, reducing β narrows the surface region of the potential. U_Λ for $\beta=\infty$ is somewhat shallower than for $\beta=2$; this difference is compensated by the smaller m_Λ^* (larger ϵ) and hence larger kinetic energy for the latter, both potentials inclusive of m_Λ^* giving similar B_Λ.

V. THE A AND ρ DEPENDENCE OF THE EFFECTIVE ΛNN POTENTIAL

Our best fits with FF require $\beta=0.1-2$, implying a ρ dependence of the effective ΛNN interaction. Equivalently, this implies an A (and l) dependence of the ΛNN strength W if the unmodified $V_{\Lambda NN}$ of Eq. (6) is used. This equivalence is quantified in Table VI. This shows the ΛNN potential energies $\langle V_{\Lambda NN}\rangle$ for the unmodified $V_{\Lambda NN}$ normalized to $W=0.02$ and obtained with Λ-core wave functions ϕ_Λ for each A,l corresponding to two of our best fits. (We confirmed that

TABLE VI. ΛNN energies and the ratios $\gamma_A(\beta)$. ΛNN potential energies $\langle V_{\Lambda NN}\rangle$ (MeV) are for $V_0=6.2$ MeV, $W=0.02$ MeV, $\beta=\infty$; the ratios $\gamma_A(\beta)$ are given by Eq. (47).

	$\langle V_{\Lambda NN}\rangle$				$\gamma_A(2)$				$\gamma_A(0.1)$			
	s	*p*	*d*	*f*	*s*	*p*	*d*	*f*	*s*	*p*	*d*	*f*
^{11}C	6.3				0.76				0.63			
^{12}C	7.6	2.1			0.82	0.62			0.71	0.43		
^{13}C	8.1	2.5			0.81	0.64			0.72	0.48		
O	9.6	3.8			0.81	0.68			0.71	0.53		
Si	15.0	8.3			0.85	0.75			0.77	0.64		
S	16.3	9.4			0.84	0.76			0.77	0.64		
Ca	17.6	11.1	6.1		0.85	0.78	0.69		0.76	0.68	0.54	
V	22.8	14.8	9.0		0.89	0.82	0.76		0.83	0.74	0.67	
Y	25.6	19.6	14.1	9.5	0.90	0.84	0.79	0.72	0.85	0.75	0.70	0.60
La	26.5	22.8	18.5	14.3	0.93	0.88	0.83	0.78	0.87	0.80	0.75	0.69
Pb	26.5	24.4	21.4	17.9	0.94	0.90	0.86	0.81	0.88	0.84	0.78	0.73

the effect of using different ϕ_Λ corresponding to different fits is small if the fits give similar B_Λ and are normalized to the same *W*.) We also show the ratios

$$\gamma_A(\beta)=\langle V^{(\beta)}_{\Lambda NN}\rangle/\langle V_{\Lambda NN}\rangle \tag{47}$$

for $\beta=0.1$ and 2. $\langle V^{(\beta)}_{\Lambda NN}\rangle$ is calculated in the same way as $\langle V_{\Lambda NN}\rangle$ but with Eq. (30) which includes $F_\beta(\rho)$. The ratio γ_A is effectively independent of *W* but depends on *A* and *l* (we suppress the *l* index) and is a measure of the effectiveness of $F_\beta(\rho)$. Thus for any given fit, obtained for some *W* and β, the strength of the unmodified dispersive $V_{\Lambda NN}$ of Eq. (6), which gives the same B_Λ is given by

$$W_A=\gamma_A(\beta)W. \tag{48}$$

γ_A has the expected behavior: for fixed β the ratio $\gamma(\beta)$ is less for smaller *A* since then the surface is relatively more important, γ_A is close to 1 for large *A*, and $F_\beta(\rho)$ is chosen so as to give $\gamma_A=1$ for nuclear matter with $\rho=0.165$; γ_A decreases for increasing *l* since the corresponding ϕ_Λ are then more sensitive to the surface; also for given *A*,*l* it is less for smaller β since then the repulsive ΛNN contribution from the surface is more strongly reduced. Table VII shows the values of $W_A(\beta)$ for $W=0.021$ averaged over the designated groups of HN (and *s* and *p*) states using the γ_A of Table VI. We use the value $W=0.021$ since this is appropriate to the best fit for $\beta=2$ shown in Table II.

For independent confirmation of the increase of the effective W_A with *A*, we obtained directly with the unmodified $V_{\Lambda NN}$ of Eq. (6) the values of W_A which give the best fits for the appropriate averages of the B_Λ of each of the groups of nuclei in Table VII. This was done for $V_0=6.2$, $\epsilon=0.255$ which correspond to our best fit for $\beta=2$. Table VII shows that for $A>13$ the value of W_A is consistent with $W_A(2)$, whereas for $A<13$ it is closer to $W_A(0.1)$.

Figure 6 also shows W_A vs $1-A^{-2/3}$, including the appropriate nuclear matter value $W=0.021$. We also show the value $W\approx 0.01$ obtained for $^5_\Lambda$He with VMC calculations for the dispersive $V_{\Lambda NN}$ of Eq. (6). Thus microscopic VMC calculations [5] using a realistic Argonne $v18$ potential [27] give $B_\Lambda=3.12\pm0.02$. (A change $\delta W=\pm0.001$ gives $\delta B_\Lambda\approx\mp0.25$.) Apart from $_\Lambda C$, which is discussed below, the plot is reasonably close to linear, consistent with a surface effect. The increase of the effective strength W_A with *A* is clearly demonstrated even apart from any uncertainties in the interpretation for $A<13$. In particular, the value for $^5_\Lambda$He is very well consistent with the trend of an increasingly repulsive dispersive ΛNN force for larger *A*. A value of *W* independent of *A* as in the best fits without FF or with a FF with $F_\beta\equiv1$ is inconsistent with $A=5$. As previously discussed, this increase in the effective repulsive ΛNN strength with *A* could arise from the changing effectiveness of $V^{2\pi}_{\Lambda NN}$ resulting from the associated ΛNN correlations and possibly also from structure effects on $V^D_{\Lambda NN}$, but these issues can only be resolved by more detailed microscopic calculations.

Modified fits with FF and the $A<13$ HN. As already remarked, the $A<13$ HN agree better with $\beta=0.1$ than with $\beta=2$. This is confirmed by calculations for just $A<13$ with both $\beta=2$ and $\beta=0.1$ (for $V_0=6.2$, $W=0.021$, $\epsilon=0.255$ appropriate to our best fit for $\beta=2$) which give a much improved fit for $\beta=0.1$ of $\chi^2=0.8$ (per B_Λ) compared to $\chi^2=4$ for $\beta=2$. Noteworthy is that all three $B_\Lambda(s)$ which were poorly fitted with $\beta=2$ are simultaneously much improved for $\beta=0.1$. We can now obtain a modified fit (shown in Fig. 1), albeit with effectively an extra parameter: V_0

TABLE VII. Effective ΛNN strengths. $\bar{A}$ is the average *A* for the designated group of HN. $W_A(\beta)$ (MeV) is W_A obtained for $W=0.021$ MeV as described in the text. $\bar{W}_A$ (MeV) is the effective value of *W* for $V_0=6.2$ MeV, $\epsilon=0.255$ obtained by direct fits to the B_Λ.

	$\bar{A}$	$W_A(2)$	$W_A(0.1)$	$\bar{W}_A$
^{11}C-^{13}C	12	0.015	0.0125	0.0135
^{16}O	16	0.016	0.013	0.0165
Si-S-Ca-V	37	0.017	0.016	0.019
Y-La-Pb	173	0.019	0.0175	0.0205

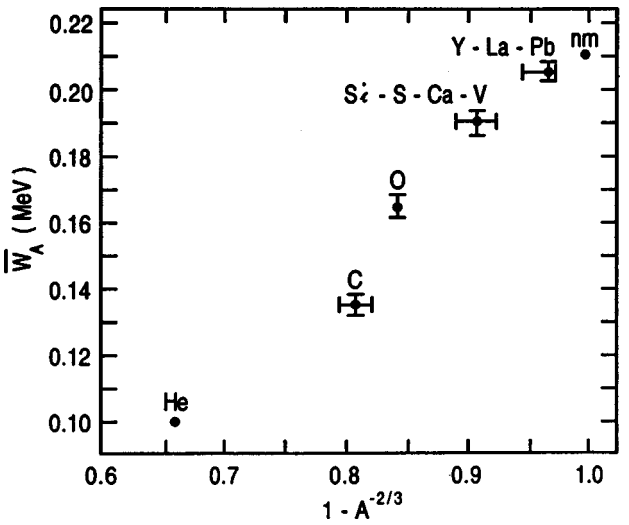

FIG. 6. The effective ΛNN strength $\bar{W}_A$ for the designated HN vs $1-A^{-2/3}$.

$=6.2$, $W=0.021$, $\epsilon=0.255$, and with $\beta=2$ for $A>13$, but with $\beta=0.1$ for $A<13$. This gives $\chi^2=1.08$, and omitting ${}^{40}_{\Lambda}\mathrm{Ca}(d)$ gives $\chi^2=0.57$ (instead of $\chi^2=1.77$, $\chi^2_1=1.33$ with $\beta=2$ for all A). Inclusion of CSB ($V_0^{\mathrm{CSB}}=-0.05$) further reduces this to $\chi^2=0.4$. These are truly excellent fits although admittedly somewhat *ad hoc* and with effectively an additional parameter and with no improvement for ${}^{40}_{\Lambda}\mathrm{Ca}(d)$.

The reduction for $A<13$ in W_A from 0.015 for $\beta=2$ to 0.125 for $\beta=0.1$ could well be due to structure effects not considered in our average approach (except indirectly through ρ) since these could be important for ${}_{\Lambda}C$ where such effects are expected to be relatively more important than for larger A. Since all the $B_\Lambda(s)$ for ${}_{\Lambda}C$ are improved simultaneously these structure effects would have to be common for all three ${}_{\Lambda}C$. A likely candidate would be a 2π-exchange ΛNN potential $V^{2\pi}_{\Lambda NN}$ (Fig. 2). In particular, this has an overall $\vec{\tau}_1\cdot\vec{\tau}_2$ factor as well as spin and tensor terms; neglecting the latter gives an overall $(\vec{\tau}_1\cdot\vec{\tau}_2)(\vec{\sigma}_1\cdot\vec{\sigma}_2)$ factor. Such terms, through the associated correlations, could possibly produce a pronounced structure dependence. Also the effect of a $(\vec{\tau}_1\cdot\vec{\tau}_2)(\vec{\sigma}_1\cdot\vec{\sigma}_2)$ factor (see, e.g., Refs. [26,29]) is strongly dependent on the spatial symmetry of the wave function and in particular on the coupling scheme. Possibly also dispersive ΛNN effects could change significantly between ${}_{\Lambda}\mathrm{C}$ and ${}^{16}_{\Lambda}\mathrm{O}$. Another mechanism which could perhaps significantly increase B_Λ is the coupling of the $(1s)$ Λ to the deformed C core nuclei, resulting in a d-state Λ component and a reduced C deformation [30]. Such questions, including the effect of ΛN spin, spin-orbit and exchange effects can only be resolved by more detailed microscopic calculations.

VI. CHARGE SYMMETRY BREAKING

The CSB potential is given by Eq. (5). This is implemented through the change $V_0\rightarrow V_0+V_0^{\mathrm{CSB}}$ in the CS ΛN potential Eq. (2). This implies CSB state independence, however, since the exchange (odd-state) contribution is relatively small, any difference between the p- and s-state CSB potentials would change our results only slightly. The change in B_Λ due to CSB is then to a good approximation

$$\Delta B_\Lambda = V_0^{\mathrm{CSB}} B'_\Lambda\left(\frac{N-Z}{A-1}\right);\quad B'_\Lambda=\frac{dB_\Lambda}{dV_0} \tag{49}$$

which is to be added to the calculated results obtained without CSB. Since ΔB_Λ is proportional to the neutron excess, we only include CSB for the four heaviest nuclei ${}^{51}_{\Lambda}\mathrm{V}(s,d)$, ${}^{89}_{\Lambda}\mathrm{Y}(s,p,d,f)$, ${}^{139}_{\Lambda}\mathrm{La}(s,p)$, ${}^{208}_{\Lambda}\mathrm{Pb}(s,p)$ making a total of $N=10$ energies, the ''heavies.'' The values of B'_Λ shown in Table VIII were obtained numerically and are almost the same for all our best-fit potentials. Also shown are the ΔB_Λ for $V_0^{\mathrm{CSB}}=-0.5$, which is close to the value preferred by analysis of the $A=4$ HN [12]. The values of ΔB_Λ are relatively small ($\simeq$2% of B_Λ for ${}^{208}_{\Lambda}\mathrm{Pb}$) but can affect the fits significantly since all the ΔB_Λ are proportional to V_0^{CSB}.

We note that the best fits without CSB are effectively unchanged if we omit the heavies. This implies that with CSB the fits including the heavies are not spuriously distorted by overweighting these if V_0^{CSB} were allowed to vary over too large a range. This can happen for poorer fits with a relatively large χ^2 which can then be strongly but spuriously reduced.

Table IX shows results for our best-fit interactions (obtained without CSB) with and without FF. $\Delta\chi^2(H)$ is the change due to a given CSB in the total $\chi^2(H)$ for all ten energies. For each interaction, $\Delta\chi^2(H)$ is shown for a range of V_0^{CSB}; also shown are the corresponding minima of $\Delta\chi^2(H)$ with the associated values of V_0^{CSB}. For the four best-fit interactions with FF and also for the bet fit for $\beta=\infty$, the minima all occur quite close to $V_0^{\mathrm{CSB}}=-0.05$, completely consistent with the value obtained from the $A=4$ HN; positive V_0^{CSB} are strongly unfavored. The optimum decreases in the total $\chi^2[\simeq\Delta\chi^2(H)/10]$ are moderate, but significantly improve the fits obtained without CSB (Tables

TABLE VIII. CSB quantities. ΔB_Λ in MeV.

			B'_Λ				$\Delta B_\Lambda(V_0^{\mathrm{CSB}}=-0.05\ \mathrm{MeV})$			
	$N-Z$	$(N-Z)/(A-1)$	s	p	d	f	s	p	d	f
${}^{51}_{\Lambda}\mathrm{V}$	4	0.08	39	30	20		0.16	0.12	0.08	
${}^{89}_{\Lambda}\mathrm{Y}$	10	0.11	42	35	28	20	0.24	0.20	0.16	0.11
${}^{139}_{\Lambda}\mathrm{La}$	24	0.17	46	40	35	28	0.40	0.35	0.30	0.24
${}^{208}_{\Lambda}\mathrm{Pb}$	43	0.21	48	44	39	34	0.50	0.46	0.41	0.35

TABLE IX. Fits with a CSB potential. $\Delta\chi^2(H)$ is the total change in $\chi^2(H)$ for all 10 heavy HN [$^{51}_{\Lambda}$V(s,p), $^{89}_{\Lambda}$Y(s,p,d,f), $^{139}_{\Lambda}$La(s,p), $^{208}_{\Lambda}$Pb(s,p)] for the listed values of $V_0^{\rm CSB}$. V_0, $V_0^{\rm CSB}$, W in MeV.

Interaction					$\Delta\chi^2(H)$				Minima	
V_0	W	β	ϵ	$V_0^{\rm CSB}=$	-0.1	-0.05	$+0.05$	$+0.1$	$V_0^{\rm CSB}$	$-\Delta\chi^2(H)$
With FF										
6.2	0.021	2.0	0.255		-1.1	-2.5	$+6.65$	$+16.9$	-0.55	2.5
6.2	0.021	0.1	0.305		$+2.7$	-0.6	$+4.6$	$+13.1$	-0.035	1.0
6.1	0.02	0.1	0.20		$+0.4$	-1.8	$+5.7$	$+15.5$	-0.045	1.8
6.15	0.02	2	0.22		-3.0	-3.5	$+7.5$	$+18.9$	-0.06	3.5
6.2	0.024	∞	0.11		-4.8	-4.4	$+8.4$	$+20.7$	-0.8	3.2
Without FF										
6.2	0.02	∞	0.35		$+26.7$	$+13.4$	-7.4	-10.8	$+0.12$	11.0
6.1	0.02	∞	0.23		$+31.2$	$+13.6$	-9.7	-16.2	$+0.15$	16.2

II and III). The resulting small χ^2 indicate that no significant improvement can be obtained by further variation of the CS parameters. A more detailed breakdown of the results shows that the principal contribution is from $\Delta\chi^2$(Pb) with its optimum at about the same $V_0^{\rm CSB}$ as for $\Delta\chi^2(H)$, and that $\Delta\chi^2$(La) and $\Delta\chi^2(Y)$ are—as expected—considerably smaller with very shallow minima at slightly larger $V_0^{\rm CSB}\approx 0$.

Without FF there is a pronounced preference for a quite large positive $V_0^{\rm CSB}\approx 0.1-0.15$. The optimum is quite large giving a very significant reduction in χ^2 (e.g., for $V_0=6.2$ from 1.5 to 0.9). The dominant contributions are now from Pb(s) and La(p) which account for most of $\Delta\chi^2$, also $\Delta\chi^2$(La) and $\Delta\chi^2(Y)$ separately have shallow minima at about the same $V_0^{\rm CSB}\approx 0.1$.

Purely on the basis of χ^2 the fits with no FF are preferred, although not strongly so, with a rather large positive $V_0^{\rm CSB}$. However for the reasons previously discussed (theoretical basis for FF, consistency with $^{5}_{\Lambda}$He) we must opt for the results with FF; these moreover confirm the CSB obtained from the $A=4$ HN which very clearly and directly favor a negative CSB interaction.

VII. CONCLUSION

We recall that in the absence of core distortion our approach is exact in the Hartree limit and is also close to the lowest order of the cluster expansion, but goes well beyond this. The fringing field due to the finite range of the ΛN and ΛNN effective interactions is an essential element which has a firm theoretical basis. We summarize our results for our best fits which were obtained by systematically searching the dependence of χ^2 on the potential parameters.

(1) A ΛN potential only, with or without space exchange, is inconsistent with the SP data, quite independently of the scattering data.

(2) The FF gives a significantly more extended and smoother SP potential U_Λ than for zero-range forces, being relatively more important for small A. With the *unmodified* dispersive $V_{\Lambda NN}$ of Eq. (6) and without exchange the FF dramatically improves the fits. Including exchange gives an excellent fit without FF for $W\approx 0.02$ MeV, and a good fit with FF for $W\approx 0.025$ MeV. However, these values are inconsistent with VMC calculations of $^{5}_{\Lambda}$He which require ≈ 0.01 MeV.

(3) The best fits with FF are obtained for $\beta\approx 0.1-2$ and correspond to a large ρ dependence $F_\beta(\rho)$ of the effective ΛNN potential of Eq. (30). This dependence translates into an A-dependent strength of the unmodified ΛNN potential, nicely consistent with $W\approx 0.01$ MeV for $^{5}_{\Lambda}$He and with ≈ 0.02 MeV for nuclear matter. The A dependence is independently confirmed by calculations with the unmodified $V_{\Lambda NN}$ of Eq. (6) in which the average strength W_A is obtained for groups of HN of different A by fitting the appropriate B_A. The increasing repulsion with A may be interpreted in terms of a combination of dispersive and two-pion exchange ΛNN potentials, the latter giving an attractive contribution for small A (as shown by VMC calculations) but one which becomes less attractive for larger A and perhaps even repulsive for heavy HN, as a consequence of the A dependence of the associated ΛNN correlations.

(4) A somewhat large attractive ΛN strength $V_0\approx 6.2$ MeV is preferred by our best fits. The exchange fraction for $V_0=6.2$ MeV is $\epsilon=0.28\pm 0.025$ and correspondingly $m^*_\Lambda(\rho_0)/m_\Lambda=0.76\pm 0.02$ and $V_p/V_s=0.45\pm 0.1$. If all values $V_0=6.15\pm 0.05$ MeV are given equal weight, then ϵ is not as well determined: $\epsilon=0.25\pm 0.05$, $m^*_\Lambda(\rho_0)/m_\Lambda=0.78\pm 0.03$, $V_p/V_s=0.5\pm 0.1$; but even these values of ϵ are considerably better than $\epsilon\approx 0.1-0.4$ obtained from Λp scattering. Without FF and for $V_0=6.15\pm 0.05$ MeV we obtain $\epsilon=0.29\pm 0.06$, $m^*_\Lambda(\rho_0)/m_\Lambda=0.76\pm 0.04$, $V_p/V_s=0.42\pm 0.12$.

(5) Because of competition between the attractive ΛN and the strongly repulsive ΛNN forces the Λ binding to nuclear matter $D(\rho)$ shows the characteristic ''saturation'' features. The maximum is at $\rho_{\rm max}\approx 0.145$ fm^{-3} for our best fits with $F_\beta=1$, both with and without FF. A density dependence $F_\beta<1$ gives a larger and sharper maximum at $\rho_{\rm max}\approx 0.125$ fm^{-3} for our best fits ($\beta=0.1$ and 2).

(6) The well depth for our best fits is $D_\Lambda\equiv D(\rho_0)\approx 29\pm 1$ MeV, very well consistent with earlier values.

(7) Charge symmetry breaking is significant for heavy hypernuclei with a large neutron excess, especially for La

and Pb for which data were obtained only recently. With a FF we obtain a negative (spin independent) CSB strength $V_0^{\rm CSB} \approx -0.05 \pm 0.02$ MeV which is completely consistent with that obtained from the $A=4$ HN (Λp more attractive than Λn) and definitely inconsistent with a positive CSB. Without a FF a quite large positive $V_0^{\rm CSB} \approx 0.1-0.15$ is strongly favored, inconsistent with $A=4$. To obtain a better estimate of $V_0^{\rm CSB}$ from the $A=4$ HN we are revisiting these with more realistic *NN* forces [31]. However we expect any changes to be quite minor since calculations for the CS ΛN potential are very little changed with use of realistic *NN* forces [5], and would not be expected to change the CSB sign. The importance of the new La and Pb data shows that more extensive data for the heavy HN could help to pin down the CSB potential.

(8) The experimental value $B_\Lambda \approx 1$ MeV for $^{40}_{\Lambda}$Ca(d) does not fit the pattern of calculated values for any of our fits with FF, the best of which give ≈3 MeV. Without FF we obtain ≈1.5 MeV quite consistent with experiment. Clearly reconsideration of the experimental value would be important. There are indications of structure effects common to the $_{\Lambda}C$ HN for which more detailed microscopic calculations would be needed.

As noted, without space exchange a FF is strongly preferred; however, the stronger dependence on ϵ without FF leads to this being preferred when exchange is included. It could be that the approximations involving the nonlocality of the exchange contributions are worse with a FF since this extends considerably outside the density distribution where $m_\Lambda^* \approx m_\Lambda$. Further study of this approximation is needed. We also note that (spherical) core distortion gives a contribution $\Delta B_\Lambda > 0$ which decreases with A, thus simulating an increasingly repulsive interaction contribution. However, estimates of ΔB_Λ (Ref. [9]) are very small $\lesssim 0.2$ MeV even for the lighter HN. For our calculations of $\Delta B_\Lambda(1s)$ we used a density functional for the core nucleus to obtain its response to the Λ. For an incompressibility constant $K=200$ MeV our most conservative (upper) estimates are $\Delta B_\Lambda \simeq 0.2$ for $A=12$ to 0.025 MeV for $A=208$, with an approximate $A^{-2/3}$ and K^{-1} dependence; but ΔB_Λ could be considerably less. For $l>0$ spherical polarization effects will be even smaller. Deformation contributions to ΔB_Λ are expected to be quite small for the nuclei we have considered, except for $_{\Lambda}C$, but need to be estimated.

We have not included a SP spin-orbit potential in our analysis. Thus the 1-s splittings observed to date (in $^{9}_{\Lambda}$Be, $^{13}_{\Lambda}$C, $^{16}_{\Lambda}$O) are not significantly different from zero ($\lesssim 0.3$ MeV). Also the relation between the SP 1-s potential and the basic (e.g., Nijmegen) OBE ΛN interaction (including the so-called ALS component) is likely to be quite as complicated as for the SP nucleon case (see, e.g., Ref. [32]), involving for example tensor components (in particular in the $\Lambda N - \Sigma N$ coupling) and/or ΛNN forces, and the effect of core excitations (Ref. [33] for $^{16}_{\Lambda}$O).

We comment briefly on the existing OBE potentials [18,19] and the associated (lowest-order) G-matrix calculations of the well depth [16,17]. All the potentials, except ND (Nijmegen D) give either a very small attractive or small repulsive odd-state (i.e., p-wave) contribution $D_p \simeq -1.0$ to 3.5 MeV ($\epsilon \simeq 0.5$). Only ND gives a significantly attractive odd-state contribution $D_p \simeq 8$ MeV (corresponding to $\epsilon \simeq 0.28$) which is comparable to those (≈7–12 MeV) obtained for our best-fit interactions (Table V). The results of the G matrix and of our FHNC calculations are not expected to differ too much for D_p (e.g., Ref. [3]). As already mentioned in Sec. IV E, the ''even-state'' G-matrix contributions are to be compared with our values of $D_s + D^{\Lambda NN}$ which are ≃16–21 MeV for our best-fit interactions (Table V), whereas the G-matrix results are ≃31–35 MeV (except for ≃24 MeV for NS0). This suggests that the G-matrix calculations are missing about 10 MeV repulsion due to higher-order (three-body) contributions, in particular from $V_{\Lambda NN}^{2\pi}$. Such a 10 MeV contribution would in particular bring the G-matrix results for ND ($D_\Lambda = 40.5$ MeV) into good agreement with two of our best-fit potentials, namely $V_0 = 6.2$ MeV, $W=0.021$ MeV, with $\beta=2$, $\epsilon=0.255$ and with $\beta=0.1$, $\epsilon=0.305$ (Table V). All the other OBE potentials, because of insufficiently attractive D_p, would then give too small $D_\Lambda \lesssim 20$ MeV. We conclude that our results show a definite preference for ND as compared with the other OBE potentials. The situation for the recently published improved Nijmegen potentials [34] remains essentially unchanged. All the new potentials give p-state potentials which are too repulsive by about 7–10 MeV than our best-fit interactions, suggesting that modifications to the p-state OBE potentials are needed. We also mention that the CSB of both the old and new potentials is similar with a pronounced spin dependence (the singlet interaction being of the wrong sign), which is in disagreement with the analysis of the data, although the spin dependence of the new potentials is less than that of the old ones. A preliminary version of the present work is in the proceedings of the HYP97 Conference [35].

ACKNOWLEDGMENTS

We thank T.-S. Harry Lee for helpful discussions and comments. This research was sponsored in part by the U.S. Department of Energy, Nuclear Physics Division, under Contract No. W-31-109-ENG-38.

[1] R. Chrien, Nucl. Phys. **A473**, 705c (1988); P. H. Pile *et al.*, Phys. Rev. Lett. **66**, 2585 (1991), for (π^+,K^+) reactions; B. Povh, Prog. Part. Nucl. Phys. **5**, 245 (1980); C. B. Dover and A. Gal, *ibid.* **12**, 171 (1984), for earlier results, in particular SEX reactions.

[2] T. Hasegawa *et al.*, Phys. Rev. C **53**, 1210 (1996).

[3] A. R. Bodmer and Q. N. Usmani, Nucl. Phys. **A477**, 621 (1988); A. R. Bodmer, Q. N. Usmani, and J. Carlson, Phys. Rev. C **29**, 684 (1984).

[4] A. A. Usmani, Phys. Rev. C **52**, 1773 (1995).

[5] S. Murali, Ph.D. thesis, Jamia Millia Islamia, New Delhi, India, 1995; Rita Sinha, Ph.D. thesis, Department of Physics,

Jamia Millia Islamia, New Delhi, India, 1999.
[6] A. A. Usmani, S. C. Pieper, and Q. N. Usmani, Phys. Rev. C **51**, 2347 (1995).
[7] Q. N. Usmani, Nucl. Phys. **A340**, 397 (1980).
[8] J. Dabrowski and W. Piechocki, Ann. Phys. (N.Y.) **126**, 317 (1980); W. Piechocki and J. Dabrowski, Acta Phys. Pol. B **12**, 475 (1981).
[9] Q. N. Usmani and A. R. Bodmer, *Condensed Matter Theories*, edited by J. W. Clark, K. A. Shoaib, and A. Sadig (Nova, Commack, New York, 1994) p. 395.
[10] A. R. Bodmer, S. Murali, and Q. N. Usmani, Nucl. Phys. **609**, 326 (1996).
[11] Q. N. Usmani, M. Sami, and A. R. Bodmer, *Condensed Matter Theories* [9], p. 381.
[12] A. R. Bodmer and Q. N. Usmani, Phys. Rev. C **31**, 1400 (1985).
[13] D. J. Millener, C. B. Dover, and A. Gal, Phys. Rev. C **38**, 2700 (1988).
[14] J. Mandal, Ph.D. thesis, Jamia Millia Islamia, New Delhi, India, 1995.
[15] M. Rufa, H. Stöcker, J. Maruhn, P.-G. Reinhard, and W. Greiner, J. Phys. G **13**, 143 (1987); M. Rufa, J. Schaffner, J. Maruhn, H. Stöcker, W. Greiner, and P.-G. Reinhard, Phys. Rev. C **42**, 2469 (1990); J. Mareš, and J. Žofka, Z. Phys. A **333**, 209 (1989); **345**, 47 (1993); R. J. Lombard, S. Marcos, and J. Mareš, Phys. Rev. C **51**, 1784 (1995); Zhong-yu Ma, J. Speth, S. Krewald, Bao-qiu Chen, and A. Reuber, Nucl. Phys. **A608**, 305 (1996); for earlier work: R. Brockmann and W. Weise, *ibid.* **A355**, 365 (1981); J. Boguta and S. Bohrmann, Phys. Lett. **102B**, 93 (1981).
[16] T. Motoba and Y. Yamamoto, Nucl. Phys. **A585**, 29c (1995); Y. Yamamoto and H. Bando, Prog. Theor. Phys. **73**, 905 (1985).
[17] Y. Yamamoto, A. Reuber, H. Himeno, S. Nagata, and T. Motoba, Czech. J. Phys. **42**, 1249 (1992); Jifa Hao, T. T. S. Kuo, A. Reuber, K. Holinde, J. Speth, and D. J. Millener, Phys. Rev. Lett. **71**, 1498 (1993); Y. Yamamoto and H. Bando, Prog. Theor. Phys. **83**, 254 (1990).
[18] M. M. Nagels, Th. A. Rijken, and J. J. de Swart, Phys. Rev. D **15**, 2547 (1977); **20**, 1633 (1979); P. M. Maessen, Th. A. Rijken, and J. J. de Swart, Phys. Rev. C **40**, 2226 (1989).
[19] R. Buttgen, K. Holinde, B. Holzenkamp, and J. Speth, Nucl. Phys. **A450**, 403c (1986); A. Reuber, K. Holinde, and J. Speth, Czech. J. Phys. **42**, 1115 (1992), and references therein; J. Speth, Proceedings of the Hypernuclear Physics Workshop, Jefferson Lab, 1995 (unpublished), p. 5.
[20] A. R. Bodmer and D. M. Rote, Nucl. Phys. **A169**, 1 (1971).
[21] S. Shinmura, Y. Akaishi, and H. Tanaka, Prog. Theor. Phys. **71**, 546 (1984).
[22] I. E. Lagaris and V. R. Pandharipande, Nucl. Phys. **A359**, 331 (1981).
[23] A. R. Bodmer, D. M. Rote, and A. L. Mazza, Phys. Rev. C **2**, 1623 (1970); J. Law, M. R. Gunye, and R. K. Bhaduri, in Proceedings of the International Conference on Hypernuclear Physics, Argonne National Laboratory, edited by A. R. Bodmer and L. G. Hyman (unpublished), p. 333
[24] J. Rozynek and J. Dabrowski, Phys. Rev. C **20**, 1612 (1979); **23**, 1706 (1981); Y. Yamamoto and H. Bando, Suppl. Prog. Theor. Phys. Suppl. **81**, 9 (1985); Y. Yamamoto, Nucl. Phys. **A450**, 275c (1986).
[25] R. K. Bhaduri, B. A. Loiseau, and Y. Nogami, Ann. Phys. (N.Y.) **44**, 57 (1967).
[26] A. Gal, Adv. Nucl. Phys. **8**, 1 (1975).
[27] R. B. Wiringa, Phys. Rev. C **43**, 1585 (1991); R. B. Wiringa, V. G. J. Stoks, and R. Schiavilla, *ibid.* **51**, 38 (1995).
[28] H. D. Vries, C. W. de Jager, and C. de Vries, At. Data Nucl. Data Tables **37**, 495 (1987).
[29] A. R. Bodmer and J. W. Murphy, Nucl. Phys. **64**, 593 (1965).
[30] T.-S. Harry Lee (private communication).
[31] Rita Sinha, Q. N. Usmani, and A. R. Bodmer (work in progress).
[32] S. C. Pieper and V. R. Pandharipande, Phys. Rev. Lett. **70**, 2541 (1993).
[33] R. H. Dalitz, D. H. Davies, T. Motoba, and D. N. Tovee, Nucl. Phys. **A625**, 71 (1997).
[34] Th. A. Rijken, V. G. J. Stoks, and Y. Yamamoto, Phys. Rev. C **59**, 21 (1999).
[35] Q. N. Usmani and A. R. Bodmer, *Proceedings of the HYP97 Conference* [Nucl. Phys. **A639**, 147c (1997)].